nanoICT School 2009

NanoPhotonics - NanoOptics - Modeling

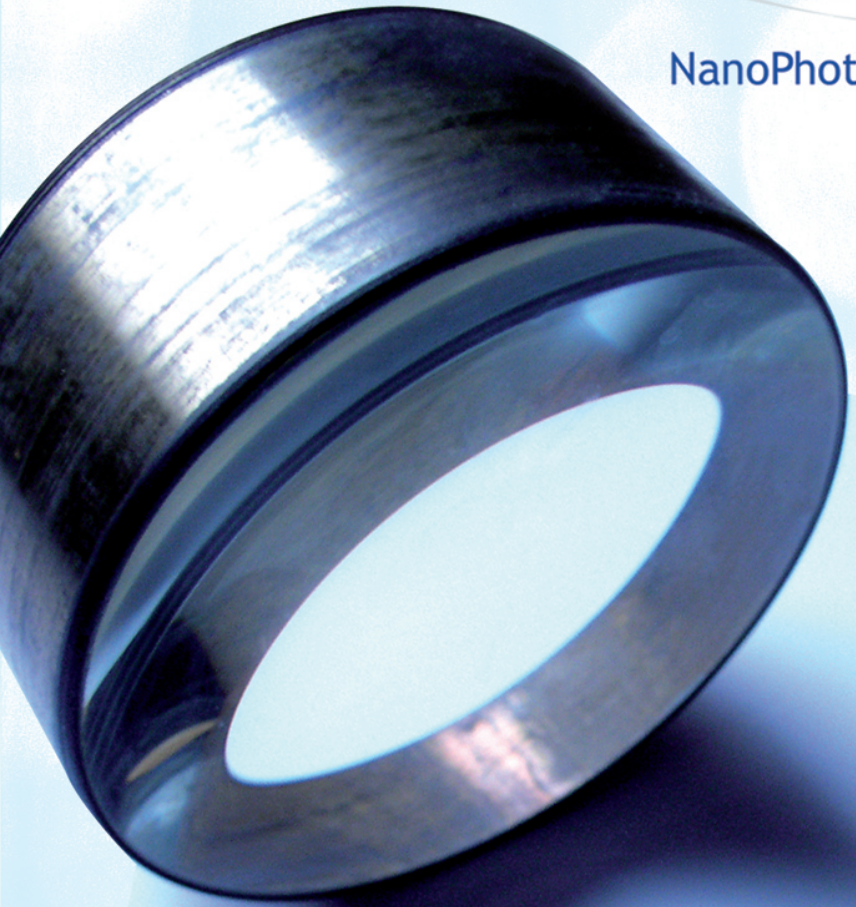

eman ta zabal zazu
universidad del país vasco
euskal herriko unibertsitatea

PHANTOMS foundation

DONOSTIA INTERNATIONAL PHYSICS CENTER
fundación D.I.P.C

CSIC
Consejo Superior de Investigaciones Científicas

CIC nanoGUNE
nanoscience cooperative research center


nanoICT
School 2009
NanoPhotonics - NanoOptics - Modeling

Depósito Legal / Spanish Legal Deposit: M-44855-2009

Nanoelectronics represent a strategic technology considering the wide range of possible applications.

Many of the potential emerging nanoelectronic applications still require substantial work in order to be transformed into marketable technology. A concerted effort must therefore be made at the European level to both understand and commercialise molecular and atomic scale technology in order to maintain a competitive advantage for Europe and keep Europe at the forefront of the next nanoelectronics revolution, a revolution beyond nanotechnology.

In order for the field of emerging nanoelectronics to continue growing exponentially worldwide and therefore lead to new commercial applications and to change the micro and nanoelectronics paradigm, it is necessary to educate new researchers who can work across traditional disciplines. The EU funded nanoICT project (nº 216165) will establish a broad array of specialised training activities to provide mainly students with interdisciplinary competences in Nanotechnology and more specifically "nano-scale ICT devices & systems" (Emerging Nanoelectronics). These initiatives will generate a new generation of high-skilled interdisciplinary scientists, indispensable to the sustainability of European excellence in the topic considered, but also educate the current working force. The main training event will be a one **post-graduate winter school on "ICT nanoscale devices**" research domains organised in collaboration with the Donostia International Physics Center (DIPC), CSIC and CIC nanoGUNE.

nanoICT School 2009
NanoPhotonics - NanoOptics - Modeling

Event format

School 1: NanoOptics and NanoPhotonics (October 26-27, 2009)
Professors: Rainer Hillenbrand (CIC nanoGUNE, Spain) / Juan Jose Saenz (UAM, Spain) / Remi Carminati (ESPCI, France) / Niek van Hulst (ICFO, Spain) / Luis Froufe (ICMM-CSIC, Spain) / Javier Aizpurua (CSIC - UPV/EHU - DIPC, Spain)

nanoICT symposium (October 28, 2009)
Invited Speakers: Rainer Hillenbrand (CIC nanoGUNE, Spain) / Juan Jose Saenz (UAM, Spain) / Remi Carminati (ESPCI, France) / Niek van Hulst (ICFO, Spain) / Uzi Landman (Georgia Tech, USA) / Stephan Roche (CEA-INAC, France) / Javier Aizpurua (CSIC - UPV/EHU - DIPC, Spain) / Pablo Ordejon (CIN2, Spain) / Luis Hueso (CIC nanoGUNE, Spain) / Yann-Michel Niquet (CEA/INAC, France) / Rafael Gutierrez (Dresden University of Technology, Germany) / Antonio Garcia Martin (IMM-CSIC, Spain) / Daniel Sanchez-Portal (CSIC - UPV/EHU – DIPC, Spain) / Luis Froufe (ICMM-CSIC, Spain)

School 2: nanoICT modeling issues (October 29-30, 2009)
Professors: Uzi Landman (Georgia Tech, USA) / Stephan Roche (CEA-INAC, France) / Rafael Gutierrez (Dresden University of Technology, Germany) / Pablo Ordejon (CIN2, Spain) / Massimo Macucci (Pisa University, Italy) / Yann-Michel Niquet (CEA/INAC, France)

nanoICT School 2009
San Sebastian – Spain / October 26-30, 2009

	Monday 26/10/2009	Tuesday 27/10/2009	Wednesday 28/10/2009	Thursday 29/10/2009	Friday 30/10/2009
A.M.	Courses	Courses	Invited Talks	Courses	Courses
	Lunch	Lunch	Lunch	Lunch	Lunch
P.M.	Courses	Courses	Invited Talks	Courses	Courses
	School 1 NanoOptics and NanoPhotonics		nanoICT one-day Symposium	School 2 nanoICT modeling issues	

nanoICT Coordination Action (nanoICT)

The nanoICT Coordination Action activities will reinforce and support the whole European Research Community in "ICT nanoscale devices" covering the following research areas expected to demonstrate unconventional solutions beyond the expected limits of CMOS technology:

1. Demonstration of new concepts for switches or memory cells
2. Demonstration of new concepts, technologies and architectures for local and chip level interconnects with substantial improvements over current solutions
3. Demonstration of radically new functionalities by the integration of blocks from a few nanometres down to the atomic scale into high added-value systems

The CA action plans will go beyond the organisation of conferences, workshops, exchange of personnel, WEB site, etc. developing the following activities:

1. Consolidation and visibility of the research community in ICT nanoscale devices
2. Mapping and benchmarking of research at European level, and its comparison with other continents
3. Identification of drivers and measures to assess research in ICT nanoscale devices, and to assess the potential of results to be taken up in industrial research
4. Coordination of research agendas and development of research roadmaps
5. Coordination of national or regional research programmes or activities, with the aim to involve funding authorities in building the ERA around this topic
6. Development of strategies for international cooperation on themes related to NanoICT

Expected impact will be the enhanced visibility, shaping and consolidation of the NanoICT research community in Europe.

Short Facts	
nanoICT	Nano-scale ICT Devices and Systems Instrument Coordination Action
EC contribution	1 Meuros
Contract number	216165
Nº of partners	12
Coordinator	Phantoms Foundation (Spain) / Antonio Correia
Start date	January 01, 2008
Duration	36 months
WEB site	**www.nanoict.org**

Organisers:

Phantoms Foundation

FET / EU

CIC nanoGUNE

Universidad del País Vasco

Donostia International Physics Center

Consejo Superior de Investigaciones Científicas

Sponsors:

nanoICT Coordination Action

FET / EU

CIC nanoGUNE

Donostia International Physics Center

Event organised in collaboration with:

nanoICT Coordination Action

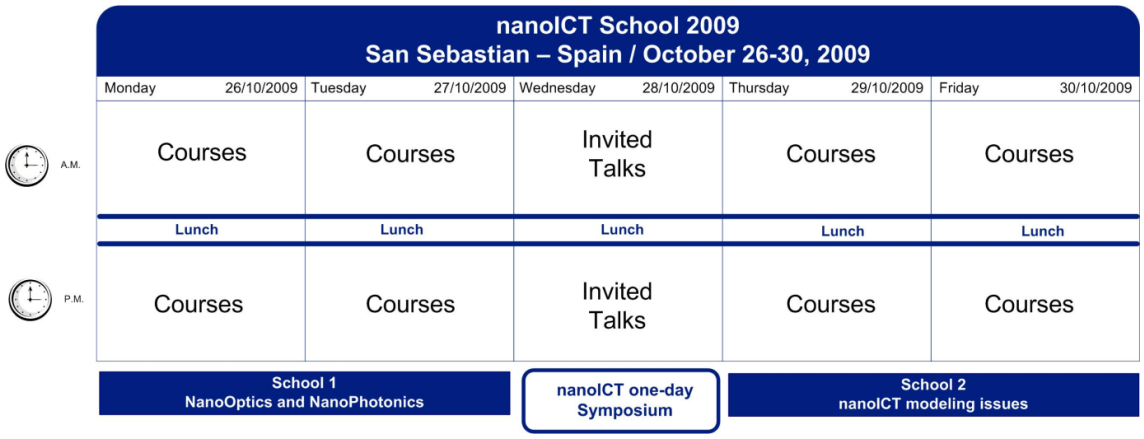

Scientific Programme - nanoICT one-day Symposium Wednesday October 28, 2009	
09:00-09:30	**Remi Carminati** (ESPCI, France)
	Nano-optics in disordered media
09:30-10:00	**Juan Jose Saenz** (UAM, Spain)
	Giant enhanced diffusion of nanoparticles in optical vortex fields
10:00-10:30	**Luis Froufe** (ICMM-CSIC, Spain)
	Threshold of a Random Laser with Cold Atoms
10:30-11:00	**Antonio Garcia-Martin** (IMM-CSIC, Spain)
	Magnetoplasmonics: an overview on the fundamentals and applications
11:00-11:30	**Coffee Break – Poster Session**
11:30-12:00	**Niek Van Hulst** (ICFO, Spain)
	Controlling photon emitters on nanometer and femtosecond scale
12:00-12:30	**Rainer Hillenbrand** (CIC nanoGUNE, Spain)
	IR and THz nanoscopy for characterizing electronic and photonic nanostructures
12:30-13:00	**Javier Aizpurua** (CSIC - UPV/EHU - DIPC, Spain)
	Metallic nanoantennas for field-enhanced spectroscopy and microscopy
13:00-13:30	**Luis Hueso** (CIC nanoGUNE, Spain)
	Spintronics with Organic Semiconductors
13:30-15:30	**Lunch (Buffet) – Poster Session**
15:30-16:00	**Yann-Michel Niquet** (CEA-INAC, France)
	Modeling the electronic, optical and transport properties of semiconductor nanowires
16:00-16:30	**Stephan Roche** (CEA-INAC, France)
	Applying magnetic fields to carbon-based low dimensional materials: from Aharonov-Bohm effects to Landau levels formations
16:30-17:00	**Pablo Ordejon** (CIN2, Spain)
	Transport properties of carbon nanotube links between graphene layers
17:00-17:30	**Coffee Break – Poster Session**
17:30-18:00	**Uzi Landman** (Georgia Tech, USA)
	Classical and quantum emergent behavior at the nanoscale
18:00-18:30	**Daniel Sanchez Portal** (CSIC - UPV/EHU - DIPC, Spain)
	Tilt angle dependence of electronic transport in molecular junctions of self-assembled alkanethiols
18:30-19:00	**Rafael Gutierrez** (Dresden University of Technology, Germany)
	Charge transport through bio-molecular wires in a solvent: Bridging molecular dynamics and model Hamiltonian approaches

School 1: NanoOptics and NanoPhotonics (October 26-27, 2009)

Professors – Alphabetical Order

Javier Aizpurua (CSIC - UPV/EHU - DIPC, Spain)
Center for Materials Physics CSIC-UPV/EHU and Donostia International Physics Center DIPC,
Paseo Manuel de Lardizabal 4, 20018 Donostia-San Sebastián, Spain (***aizpurua*@*ehu.es***)

Basic aspects of optical response in nanostructures
Course 1: Optical response in metallic nanoantennas
Course 2: Optical response in semiconductor quantum dots

Remi Carminati (ESPCI, France)
Institut Langevin, ESPCI ParisTech, CNRS
10, rue Vauquelin, 75231 Paris Cedex 05, France (**remi.carminati@espci.fr**)

Single dipole emitters in nanostructured environments
Course 1: Dipole radiation: From classical to quantum
Course 2: Single-molecule fluorescence in complex environments

Luis Froufe (ICMM-CSIC, Spain)
Instituto de Ciencia de Materiales de Madrid (ICMM) - CSIC.
Sor Juana Inés de la Cruz 3, Cantoblanco 28049, Spain (**luis.froufe@icmm.csic.es**)

Photonic crystals
Course 1: Introduction
Course 2: Light emission and transport

Rainer Hillenbrand (CIC nanoGUNE Consolider, Spain)
CIC nanoGUNE Consolider
Tolosa Hiribidea 76, E-20018 Donostia - San Sebastian, Spain (**r.hillenbrand@nanogune.eu**)

Basics and applications of near-field optical microscopy

Juan Jose Saenz (Universidad Autonoma de Madrid, Spain)
Moving Light and Electrons (Mole) Group, Univ. Autónoma de Madrid, Spain
(**juanjo.saenz@uam.es**)

Electromagnetic and light forces on small particles
Course 1: Scattering, absorption and radiation pressure
Course 2: Non-conservative light forces

Niek van Hulst (ICFO, Spain)
ICFO - Institut de Ciències Fotòniques,Parc Mediterrani de la Tecnologia
Av. del Canal Olímpic s/n 08860 Castelldefels (Barcelona), Spain. (**niek.vanhulst@icfo.es**)

Course 1: Single molecules & single photon emitters
Course 2: Adressing the nanoscale by far and near field optical methods

Scientific Programme - nanoICT School 1 (NanoOptics – NanoPhotonics)	
Monday October 26, 2009	
08:30-09:00	**Registration**
09:00-09:45	**Remi Carminati** (ESPCI, France)
	Single dipole emitters in nanostructured environments *Course 1: Dipole radiation: From classical to quantum*
09:45-10:15	**Discussion**
10:15-11:00	**Luis Froufe** (ICMM-CSIC, Spain)
	Photonic crystals *Course 1: Introduction*
11:00-11:30	**Discussion**
11:30-12:00	**Coffee Break – Poster Session**
12:00-12:45	**Juan Jose Saenz** (Universidad Autonoma de Madrid, Spain)
	Electromagnetic and light forces on small particles *Course 1: Scattering, absorption and radiation pressure*
12:45-13:15	**Discussion**
13:15-15:00	**Lunch**
15:00-15:45	**Remi Carminati** (ESPCI, France)
	Single dipole emitters in nanostructured environments *Course 2: Single-molecule fluorescence in complex environments*
15:45-16:15	**Discussion**
16:15-17:00	**Luis Froufe** (ICMM-CSIC, Spain)
	Photonic crystals *Course 2: Light emission and transport*
17:00-17:30	**Discussion**
17:30-18:00	**Coffee Break – Poster Session**
18:00-18:45	**Juan Jose Saenz** (Universidad Autonoma de Madrid, Spain)
	Electromagnetic and light forces on small particles *Course 2: Non-conservative light forces*
18:45-19:15	**Discussion**

Scientific Programme - nanoICT School 1 (NanoOptics – NanoPhotonics)	
Tuesday October 27, 2009	
09:00-09:45	**Rainer Hillenbrand** (CIC nanoGUNE, Spain)
	Basics and applications of near-field optical microscopy (1)
09:45-10:15	**Discussion**
10:15-11:00	**Javier Aizpurua** (CSIC - UPV/EHU - DIPC, Spain)
	Basic aspects of optical response in nanostructures *Course 1: Optical response in metallic nanoantennas*
11:00-11:30	**Discussion**
11:30-12:00	**Coffee Break – Poster Session**
12:00-12:45	**Niek van Hulst** (ICFO, Spain)
	Course 1: Single molecules & single photon emitters
12:45-13:15	**Discussion**
13:15-15:00	**Lunch**
15:00-15:45	**Rainer Hillenbrand** (CIC nanoGUNE, Spain)
	Basics and applications of near-field optical microscopy (2)
15:45-16:15	**Discussion**
16:15-17:00	**Javier Aizpurua** (CSIC - UPV/EHU - DIPC, Spain)
	Basic aspects of optical response in nanostructures *Course 2: Optical response in semiconductor quantum dots*
17:00-17:30	**Discussion**
17:30-18:00	**Coffee Break – Poster Session**
18:00-18:45	**Niek van Hulst** (ICFO, Spain)
	Course 2: Adressing the nanoscale by far and near field optical methods
18:45-19:15	**Discussion**

Posters (14)

Name	Surname	Institution	Country	Topic / School
Nicklas	**Anttu**	Lund University	Sweden	NanoOptics-NanoPhotonics
Coupling of light into nanowire arrays and subsequent absorption				
Francisco Javier	**Aparicio Rebollo**	Instituto de Ciencias de Materiales de Sevilla	Spain	NanoOptics-NanoPhotonics
Luminescent plasma nanocomposites for the fabrication of photonic sensing devices				
Jorge	**Fernández Torrado**	Instituto de Microelectrónica de Madrid (CNM-CSIC)	Spain	NanoOptics-NanoPhotonics
Interaction between LSP and SPP in magnetoplasmonic structures				
Prem Kumar	**Kandaswamy**	CEA-Grenoble, INAC/SP2M	France	NanoOptics-NanoPhotonics
III-N nanostructures for Intersubband optoelectronics				
Nicolas	**Large**	Centro Mixto de Física de Materiales CSIC-UPV/EHU & DIPC	Spain	NanoOptics-NanoPhotonics
Acousto-plasmonic hot spots in metallic nano-objects				
Luis Enrique	**Muñoz**	IMM-CNM-CSIC	Spain	NanoOptics-NanoPhotonics
Two-dimensional surface emitting photonic crystal laser with hybrid triangular-graphite structure				
David	**Papencordt**	University of Mainz	Germany	NanoOptics-NanoPhotonics
Spectroscopy of thin molecular films under ultrahigh vacuum conditions using an optical nanofiber				
Olalla	**Pérez-González**	DIPC - University of the Basque Country	Spain	NanoOptics-NanoPhotonics
Optical Spectroscopy of Molecular Junctions in Plasmonic Cavities				
Juan Ramón	**Sánchez Valencia**	Instituto de Ciencia de Materiales de Sevilla	Spain	NanoOptics-NanoPhotonics
Light Processing of Nanoporous Semiconducting Oxides for the Fabrication of Optically Active Thin Films				
Martin	**Schnell**	Asociación CIC nanoGUNE	Spain	NanoOptics-NanoPhotonics
Control of local near fields in optical antennas by load engineering				
Ariane	**Stiebeiner**	University of Mainz	Germany	NanoOptics-NanoPhotonics
Ultra-sensitive fluorescence spectroscopy of isolated surface-adsorbed molecules using an optical nanofiber				
Johannes	**Stiegler**	CIC nanoGUNE	Spain	NanoOptics-NanoPhotonics
Nanoscale infrared near-field mapping of free-carrier concentration in single semiconductor nanowires				
Francisco Javier	**Valdivia-Valero**	ICMM-CSIC	Spain	NanoOptics-NanoPhotonics
Supertransmission and light concentration at nanoscale				
Alan	**Vitrey**	Instituto de Microelectrónica de Madrid (CNM-CSIC)	Spain	NanoOptics-NanoPhotonics
Towards Near Field Characterization of Plasmonic and Magnetoplasmonic Nanostructures				

School 2: nanoICT modelling issues (October 29-30, 2009)

Professors – Alphabetical Order

Rafael Gutierrez (Dresden University of Technology, Germany)
Institute for Materials Science, Dresden University of Technology, 01062 Dresden, Germany. (**rafael.gutierrez@tu-dresden.de**)

Modeling charge and phonon transport at the nanoscale
Course 1: Charge and phonon transport in single molecules: thermoelectricity and mechanical effects at the molecular scale
Course 2: Charge propagation and dynamics in biomolecular systems

Uzi Landman (Georgia Tech, USA)
Georgia Institute of Technology, School of Physics, 837 State Street Atlanta, Georgia 30332-0430, U.S.A **(uzi.landman@physics.gatech.edu**)

Microscopic simulations of classical and quantum phenomena at the nanoscale
Course 1: Methodologies and practice I
Course 2: Methodologies and practice II

Massimo Macucci (Pisa University, Italy)
Universita' di Pisa, Dipartimento di Ingegneria dell'Informazione , Via G. Caruso 16. 56122-Pisa, Italy. (**m.macucci@mercurio.iet.unipi.it**)

Transport and Noise in Nanoelectronic Devices
Course 1: Numerical techniques for the simulation of transport in nanoscale devices
Course 2: Numerical simulation and measurement of noise in nanodevices

Yann-Michel Niquet (CEA/INAC, France)
CEA/INAC, 17 rue des Martyrs, 38054 Grenoble Cedex 9, France (**yniquet@cea.fr**)

Modeling the electronic, optical and transport properties of semiconductor nanowires

Pablo Ordejon (CIN2, Spain)
CIN2, ETSE,Campus UAB, Building Q - 2nd Floor, 08193 Bellaterra, Spain (**pablo.ordejon@cin2.es**)

Simulations of nanoscale phenomena with SIESTA
Course 1: Fundamentals
Course 2: Advanced concepts and applications

Stephan Roche (CEA-INAC, France)
CIN2 (ICN-CSIC), Campus UAB, Bellaterra (Barcelona), Spain
CEA, INAC, SP2M, L_sim, Grenoble, France (**stephan.roche@cea.fr**)

Modelling mesoscopic charge transport in nanomaterials
Course 1: Introduction to efficient order N computational transport methodologies
Course 2: Applications to carbon nanotubes and graphene based materials

Scientific Programme - nanoICT School 2 (Modeling) Thursday October 29, 2009	
09:00-09:45	**Rafael Gutierrez** (Dresden University of Technology, Germany)
	Modeling charge and phonon transport at the nanoscale *Course 1: Charge and phonon transport in single molecules: thermoelectricity and mechanical effects at the molecular scale*
09:45-10:15	**Discussion**
10:15-11:00	**Stephan Roche** (CEA-INAC, France)
	Modeling mesoscopic charge transport in nanomaterials *Course 1: Introduction to efficient order N computational transport methodologies*
11:00-11:30	**Discussion**
11:30-12:00	**Coffee Break – Poster Session**
12:00-12:45	**Uzi Landman** (Georgia Tech, USA)
	Microscopic simulations of classical and quantum phenomena at the nanoscale *Course 1: Methodologies and practice I*
12:45-13:15	**Discussion**
13:15-15:00	**Lunch**
15:00-15:45	**Rafael Gutierrez** (Dresden University of Technology, Germany)
	Modeling charge and phonon transport at the nanoscale *Course 2: Charge propagation and dynamics in biomolecular systems*
15:45-16:15	**Discussion**
16:15-17:00	**Stephan Roche** (CEA-INAC, France)
	Modeling mesoscopic charge transport in nanomaterials *Course 2: Applications to carbon nanotubes and graphene based materials*
17:00-17:30	**Discussion**
17:30-18:00	**Coffee Break – Poster Session**
18:00-18:45	**Uzi Landman** (Georgia Tech, USA)
	Microscopic simulations of classical and quantum phenomena at the nanoscale *Course 2: Methodologies and practice II*
18:45-19:15	**Discussion**

Scientific Programme - nanoICT School 2 (Modeling) Friday October 30, 2009	
09:00-09:45	**Pablo Ordejon** (CIN2, Spain)
	Simulations of nanoscale phenomena with SIESTA *Course 1: Fundamentals*
09:45-10:15	**Discussion**
10:15-11:00	**Yann-Michel Niquet** (CEA-INAC, France)
	Modeling the electronic, optical and transport properties of semiconductor nanowires (1)
11:00-11:30	**Discussion**
11:30-12:00	**Coffee Break – Poster Session**
12:00-12:45	**Massimo Macucci** (Pisa University, Italy)
	Transport and Noise in Nanoelectronic Devices *Course 1: Numerical techniques for the simulation of transport in nanoscale devices*
12:45-13:15	**Discussion**
13:15-15:00	**Lunch**
15:00-15:45	**Pablo Ordejon** (CIN2, Spain)
	Simulations of nanoscale phenomena with SIESTA *Course 2: Advanced concepts and applications*
15:45-16:15	**Discussion**
16:15-17:00	**Yann-Michel Niquet** (CEA-INAC, France)
	Modeling the electronic, optical and transport properties of semiconductor nanowires (2)
17:00-17:30	**Discussion**
17:30-18:00	**Coffee Break – Poster Session**
18:00-18:45	**Massimo Macucci** (Pisa University, Italy)
	Transport and Noise in Nanoelectronic Devices *Course 2: Numerical simulation and measurement of noise in nanodevices*
18:45-19:15	**Discussion**

Posters (12)

Name	Surname	Institution	Country	Topic / School
Alfonso	**Alarcón Pardo**	Universitat Autonoma de Barcelona	Spain	Modeling
Explicit computation of Bohm velocity for N-electrons in open quantum systems				
Guillem	**Albareda**	Universitat Autonoma de Barcelona	Spain	Modeling
Coulomb-correlations in the electric power of nanoscale open systems				
Thomas	**Brumme**	TU Dresden	Germany	Modeling
Modeling switching in STM molecular junctions				
Thales	**de Oliveira**	CIC nanoGUNE Consolider	Spain	Modeling
Amplitude- and phase-resolved optical near fields of propagating surface plasmons on extended and nanostructured thin films				
Szymon	**Godlewski**	Jagiellonian University	Poland	Modeling
Atomically structured metallic nanowires on the KBr passivated InSb surface				
Nicolas	**Leconte**	Université Catholique de Louvain (UCL)	Belgium	Modeling
Electronic and transport properties of graphene due to its functionalization using dopants, chemical groups or metallic clusters				
Wu	**Li**	TU Dresden	Germany	Modeling
Study the phonon transport by using the real space Kubo method				
Pedro David	**Manrique Charry**	TU Dresden	Germany	Modeling
Quantum master equation for the study of electronic transport in organic systems.				
José Luis	**Padilla**	Universidad de Granada	Spain	Modeling
Study and simulations of SB-MOSFETs on SOI substrates				
Miguel Angel	**Pérez Osorio**	CIN2: CSIC-ICN	Spain	Modeling
Formation energy of charge states of nitrogen and oxygen vacancies in anatase TiO2: an ab initio study				
Massimo	**Totaro**	University of Pisa	Italy	Modeling
Noise properties of mesoscopic devices with realistic potential profile				
Dawid	**Toton**	Jagiellonian University	Poland	Modeling
Theoretical study of PTCDA molecules adsorbed on InSb(001) surface				

Index

Alphabetical Order

Invited Speakers (nanoICT Symposium) – Alphabetical Order

Name	Surname	Institution	Country	Page
Javier	**Aizpurua**	CSIC - UPV/EHU - DIPC	Spain	p. 1
Metallic nanoantennas for field-enhanced spectroscopy and microscopy				
Remi	**Carminati**	ESPCI	France	p. 3
Nano-optics in disordered media				
Luis	**Froufe**	ICMM-CSIC	Spain	p. 5
Threshold of a Random Laser with Cold Atoms				
Antonio	**Garcia-Martin**	IMM-CSIC	Spain	p. 7
Magnetoplasmonics: an overview on the fundamentals and applications				
Rafael	**Gutierrez**	Dresden University of Technology	Germany	p. 9
Charge transport through bio-molecular wires in a solvent: Bridging molecular dynamics and model Hamiltonian approaches				
Rainer	**Hillenbrand**	CIC nanoGUNE	Spain	p. 11
IR and THz nanoscopy for characterizing electronic and photonic nanostructures				
Luis	**Hueso**	CIC nanoGUNE	Spain	p. 13
Spintronics with Organic Semiconductors				
Uzi	**Landman**	Georgia Tech.	USA	--
Classical and quantum emergent behavior at the nanoscale				
Yann-Michel	**Niquet**	CEA-INAC	France	p. 15
Modeling the electronic, optical and transport properties of semiconductor nanowires				
Pablo	**Ordejon**	CIN2	Spain	p. 17
Transport properties of carbon nanotube links between graphene layers				
Stephan	**Roche**	CEA-INAC	France	p. 19
Applying magnetic fields to carbon-based low dimensional materials: from Aharonov-Bohm effects to Landau levels formations				
Juan Jose	**Saenz**	Universidad Autonoma de Madrid	Spain	p. 21
Giant enhanced diffusion of nanoparticles in optical vortex fields				
Daniel	**Sanchez-Portal**	CSIC - UPV/EHU - DIPC	Spain	p. 23
Tilt angle dependence of electronic transport in molecular junctions of self-assembled alkanethiols				
Niek	**Van Hulst**	ICFO	Spain	p. 25
Controlling photon emitters on nanometer and femtosecond scale				

Posters (26) – Alphabetical Order

Name	Surname	Institution	Country	Page
Alfonso	**Alarcón Pardo**	Universitat Autonoma de Barcelona	Spain	p. 29
Explicit computation of Bohm velocity for N-electrons in open quantum systems ***(Modeling)***				
Guillem	**Albareda**	Universitat Autonoma de Barcelona	Spain	p. 31
Coulomb-correlations in the electric power of nanoscale open systems ***(Modeling)***				
Nicklas	**Anttu**	Lund University	Sweden	p. 33
Coupling of light into nanowire arrays and subsequent absorption ***(NanoOptics-NanoPhotonics)***				
Francisco Javier	**Aparicio Rebollo**	Instituto de Ciencias de Materiales de Sevilla	Spain	p. 35
Luminescent plasma nanocomposites for the fabrication of photonic sensing devices ***(NanoOptics-NanoPhotonics)***				
Thomas	**Brumme**	TU Dresden	Germany	p. 37
Modeling switching in STM molecular junctions ***(Modeling)***				
Thales	**de Oliveira**	CIC nanoGUNE Consolider	Spain	p. 39
Amplitude- and phase-resolved optical near fields of propagating surface plasmons on extended and nanostructured thin films ***(Modeling)***				
Jorge	**Fernández Torrado**	Instituto de Microelectrónica de Madrid (CNM-CSIC)	Spain	p. 41
Interaction between LSP and SPP in magnetoplasmonic structures ***(NanoOptics-NanoPhotonics)***				
Szymon	**Godlewski**	Jagiellonian University	Poland	p. 43
Atomically structured metallic nanowires on the KBr passivated InSb surface ***(Modeling)***				
Prem Kumar	**Kandaswamy**	CEA-Grenoble, INAC/SP2M	France	p. 45
III-N nanostructures for Intersubband optoelectronics ***(NanoOptics-NanoPhotonics)***				
Nicolas	**Large**	Centro Mixto de Física de Materiales CSIC-UPV/EHU & DIPC	Spain	p. 47
Acousto-plasmonic hot spots in metallic nano-objects ***(NanoOptics-NanoPhotonics)***				
Nicolas	**Leconte**	Université Catholique de Louvain (UCL)	Belgium	p. 49
Electronic and transport properties of graphene due to its functionalization using dopants, chemical groups or metallic clusters ***(Modeling)***				
Wu	**Li**	TU Dresden	Germany	p. 51
Study the phonon transport by using the real space Kubo method ***(Modeling)***				
Pedro David	**Manrique Charry**	TU Dresden	Germany	p. 53
Quantum master equation for the study of electronic transport in organic systems ***(Modeling)***				

Posters (14) – School 1 (NanoOptics and NanoPhotonics)
Alphabetical Order

Name	Surname	Institution	Country	Page
Nicklas	**Anttu**	Lund University	Sweden	p. 33
Coupling of light into nanowire arrays and subsequent absorption				
Francisco Javier	**Aparicio Rebollo**	Instituto de Ciencias de Materiales de Sevilla	Spain	p. 35
Luminescent plasma nanocomposites for the fabrication of photonic sensing devices				
Jorge	**Fernández Torrado**	Instituto de Microelectrónica de Madrid (CNM-CSIC)	Spain	p. 41
Interaction between LSP and SPP in magnetoplasmonic structures				
Prem Kumar	**Kandaswamy**	CEA-Grenoble, INAC/SP2M	France	p. 45
III-N nanostructures for Intersubband optoelectronics				
Nicolas	**Large**	Centro Mixto de Física de Materiales CSIC-UPV/EHU & DIPC	Spain	p. 47
Acousto-plasmonic hot spots in metallic nano-objects				
Luis Enrique	**Muñoz**	IMM-CNM-CSIC	Spain	p. 55
Two-dimensional surface emitting photonic crystal laser with hybrid triangular-graphite structure				
David	**Papencordt**	University of Mainz	Germany	p. 59
Spectroscopy of thin molecular films under ultrahigh vacuum conditions using an optical nanofiber				
Olalla	**Pérez-González**	DIPC - University of the Basque Country	Spain	p. 63
Optical Spectroscopy of Molecular Junctions in Plasmonic Cavities				
Juan Ramón	**Sánchez Valencia**	Instituto de Ciencia de Materiales de Sevilla	Spain	p. 65
Light Processing of Nanoporous Semiconducting Oxides for the Fabrication of Optically Active Thin Films				
Martin	**Schnell**	Asociación CIC nanoGUNE	Spain	p. 67
Control of local near fields in optical antennas by load engineering				
Ariane	**Stiebeiner**	University of Mainz	Germany	p. 69
Ultra-sensitive fluorescence spectroscopy of isolated surface-adsorbed molecules using an optical nanofiber				
Johannes	**Stiegler**	CIC nanoGUNE	Spain	p. 71
Nanoscale infrared near-field mapping of free-carrier concentration in single semiconductor nanowires				
Francisco Javier	**Valdivia-Valero**	ICMM-CSIC	Spain	p. 77
Supertransmission and light concentration at nanoscale				
Alan	**Vitrey**	Instituto de Microelectrónica de Madrid (CNM-CSIC)	Spain	p. 79
Towards Near Field Characterization of Plasmonic and Magnetoplasmonic Nanostructures				

Posters (12) – School 2 (Modeling issues for nanoICT)
Alphabetical Order

Name	Surname	Institution	Country	Page
Alfonso	**Alarcón Pardo**	Universitat Autonoma de Barcelona	Spain	p. 29
Explicit computation of Bohm velocity for N-electrons in open quantum systems				
Guillem	**Albareda**	Universitat Autonoma de Barcelona	Spain	p. 31
Coulomb-correlations in the electric power of nanoscale open systems				
Thomas	**Brumme**	TU Dresden	Germany	p. 37
Modeling switching in STM molecular junctions				
Thales	**de Oliveira**	CIC nanoGUNE Consolider	Spain	p. 39
Amplitude- and phase-resolved optical near fields of propagating surface plasmons on extended and nanostructured thin films				
Szymon	**Godlewski**	Jagiellonian University	Poland	p. 43
Atomically structured metallic nanowires on the KBr passivated InSb surface				
Nicolas	**Leconte**	Université Catholique de Louvain (UCL)	Belgium	p. 49
Electronic and transport properties of graphene due to its functionalization using dopants, chemical groups or metallic clusters				
Wu	**Li**	TU Dresden	Germany	p. 51
Study the phonon transport by using the real space Kubo method				
Pedro David	**Manrique Charry**	TU Dresden	Germany	p. 53
Quantum master equation for the study of electronic transport in organic systems.				
José Luis	**Padilla**	Universidad de Granada	Spain	p. 57
Study and simulations of SB-MOSFETs on SOI substrates				
Miguel Angel	**Pérez Osorio**	CIN2: CSIC-ICN	Spain	p. 61
Formation energy of charge states of nitrogen and oxygen vacancies in anatase TiO2: an ab initio study				
Massimo	**Totaro**	University of Pisa	Italy	p. 73
Noise properties of mesoscopic devices with realistic potential profile				
Dawid	**Toton**	Jagiellonian University	Poland	p. 75
Theoretical study of PTCDA molecules adsorbed on InSb(001) surface				

Abstracts – Invited Speakers

Alphabetical Order

nanoICT Symposium

Metallic nanoantennas for field-enhanced spectroscopy and microscopy

Javier Aizpurua, Aitzol García-Etxarri, Nicolas Large, Olalla Pérez, Alejandro Reyes
Center for Materials Physics CSIC-UPV/EHU and Donostia International Physics Center DIPC, Paseo Manuel de Lardizabal 4, 20018 Donostia-San Sebastián, Spain
aizpurua@ehu.es

Optical antennas are nanoscale metallic structures which act as effective receivers, transmitters and receivers of visible light. These nanoatennas show the ability to focus electromagnetic radiation into tiny spots of nanometer-scale dimensions allowing for more effective field-enhanced visible spectroscopies such as in surface-enhanced Raman spectroscopy (SERS). A brief review on the basics of the optical response of these optical nanoantennas will be presented, with examples of the optical response in different canonical nanostructures such as metallic nanorings [1], nanorods [2], nanowires [3], dimers [4] or nanoshells [5] which are commonly used as optical nanoantennas.

We will address the use of optical nanoantennas in a variety of spectroscopy and microscopy techniques. In particular, the use of $\lambda/2$ nanorod-like gold nanoantennas will be described in detail. By engineering the length of the rod-like nanoantennas, it is possible to extend the field enhancement capability into the infrared range of the spectrum (as shown in Fig. 1 (a) for a micron-sized nanoantenna) to perform direct surface-enhanced infrared absorption (SEIRA) [6]. With use of this concept, we show that it is possible to obtain direct IR spectral information of a few thousand molecules deposited on the antenna (see Fig. 1(b)). Another option to engineer the optical response of a nanoantenna relies on the manipulation of the antenna gap. We show theoretically and experimentally the modification of the optical response of nanoatennas as a function of the thickness of the antenna gap, bridging together concepts of optics and circuit theory [7].

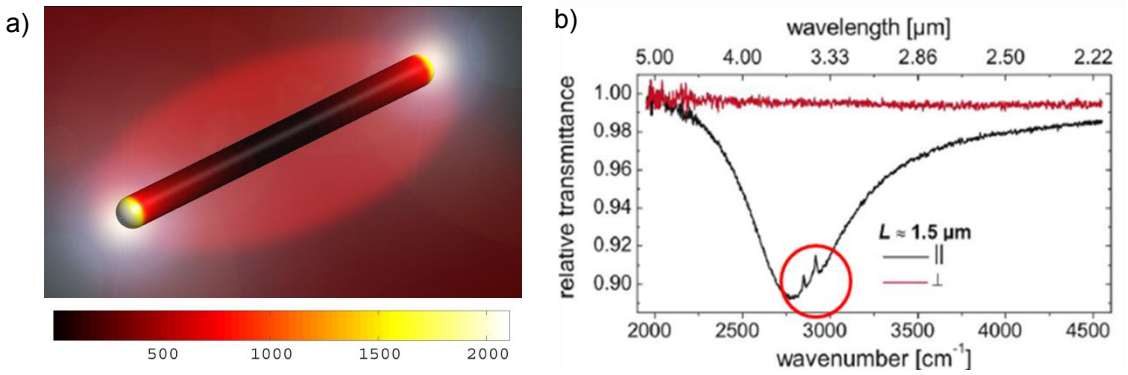

Figure 1: *(a) Near-field around an infrared nanoantenna of length L=1.3 μm when illuminated resonantly with wavelength λ=3.41 μm. (b) Transmission spectroscopy of two molecular fingerprints (marked as a red circle), when the molecules are deposited on top of an antenna similar to that in (a).*

The interaction between tip and sample in scattering-type near field optical microscopy (s-SNOM) can also be understood as an antenna effect due to the interaction of tip and sample. This near-field interaction allows for direct mapping of near-field patterns with nanoscale resolution with use of radiation from the visible to the Terahertz [8]. Examples of nanoscopy for each range of the spectrum will be presented. Another spectroscopy where the role of plasmonic resonances plays an important role is Raman-Brillouin scattering of single metallic nano-objects. The interaction between the vibrations of a metallic nano-object and the plasmons induced on it determine the activation and deactivation of certain vibrational modes in the Raman scattering. We

analyse in detail how the presence of geometrical indentations and cavities in optical nanoantennas localizes the electromagnetic fields at the indentations (see Fig. 2 (a)). Following the variations of the near-field for a particular vibrational mode (Fig. 2(b)), we can address the modulation of the near-field (Fig. 2(c)), and determine how strongly the field in the cavities and in the indentations is modulated. For certain vibrational modes such as the breathing-like mode in silver nanocolumns, these "acousto-plasmonic hot spots" produce breaking of Raman selection rules with activation of anomalous vibrational modes in Raman spectroscopy.

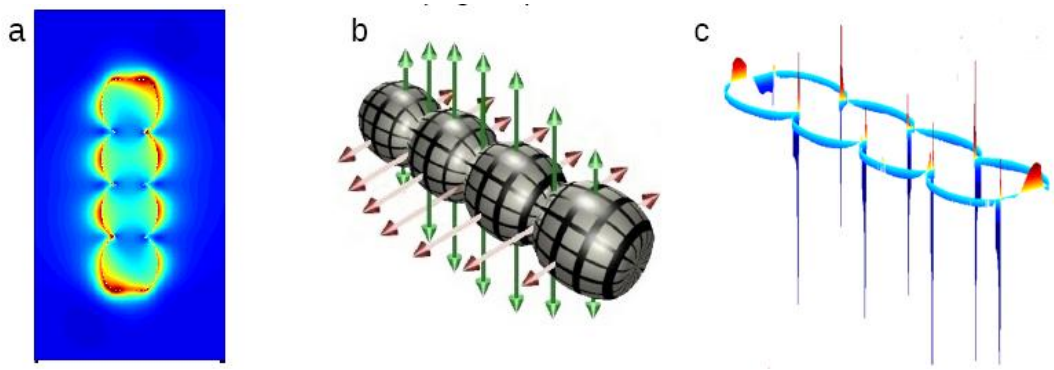

Figure 2: *(a) Near-field map around a silver nanocolumn presenting indentations (b) Breathing-like vibrational mode of the same nanocolumn, and (c) Modulation of the near-field around the nanocolumn surface for the breathing-like vibrational mode in (b). Strong "acousto-plasmonic hot spots" can be observed at the indentations, producing Raman selection rules breaking. The nanocolumn is 10 nm long, 2 nm wide and the wavelength of the incident light is* λ*=413nm.*

To illustrate the wide range of applications of plasmonic interactions in totally different systems, we will conclude by analysing the forces originated from the excitation of plasmons by the fast electron beam in Scanning Transmission Electron Microscopy (STEM). Our model calculations show that metallic nanoparticles experience attractive or repulsive forces as a function of the position of the electron beam. This ability to manipulate the forces on the particles can be used in gold nanoparticles for example to produce coalescence.

From the overview and the examples shown here, it is straightforward to conclude that an understanding of the interactions occurring at the optical nanoantennas in such a variety of systems, and the knowledge on the electromagnetic response occurring in the different spectroscopy and microscopy configurations are crucial to engineer and design plasmonic devices for improved detection and controlled optical response.

References

[1] J. Aizpurua *et al*. Phys. Rev. Lett. **90** (2003) 057401.
[2] J. Aizpurua *et al*. Phys. Rev. B. **71** (2005) 235420.
[3] F. Neubrech *et al.* Appl. Phys. Lett. **89** (2006) 253104.
[4] I. Romero *et al*. Optics Express **14** (2006) 9988.
[5] B. Lassiter *et al.* Nano Letters **8** (2008) 1212.
[6] F. Neubrech *et al*. Phys. Rev. Lett. **101** (2008) 157403.
[7] M. Schnell *et al.* Nature Photonics **3** (2009) 287.
[8] A. Cvitkovic *et al*. Phys. Rev. Lett. **97** (2006) 060801.

Nano-optics in disordered media

Rémi Carminati

Institut Langevin, ESPCI ParisTech, CNRS
10, rue Vauquelin, 75231 Paris Cedex 05, France
remi.carminati@espci.fr

The development of near-field optics, on both the technical and fundamental aspects, has allowed to image confined fields on scales on the order of 10-100 nm in the visible and infrared spectrum. Beyond imaging applications, nano-optics has emerged, in which the *control* of optical fields at subwavelength scale is a central issue. The control of local fields permits, for example, to act on the fluorescence dynamics of isolated emitters.

In this talk, we will address the issues of light emission and focusing in complex (disordered) media, and at subwavelength scale. We will discuss molecular fluorescence in scattering and absorbing media, and show how the fluorescence lifetime is modified due to near-field interactions [1,2]. In the regime of multiple scattering, we will show how the photonic density of states is connected to the scattering mean free path [3]. We will discuss the possibility of focusing light through or inside a strongly scattering medium, with a spatial resolution beyond the diffraction limit [4,5]. These results suggest novel approaches for imaging in complex media and for the engineering of photonic systems based on disordered materials.

Ackowledgments

I would like to acknowledge L. Froufe, R. Pierrat and C. Vandenbem who are at the origin of many results presented in this talk.

References

[1] L.S. Froufe-Pérez, R. Carminati and J.J. Sáenz, Phys. Rev. A **76**, 013835 (2007).
[2] L.S. Froufe-Pérez and R. Carminati, Phys. Stat. Sol. (a) **201**, 1258 (2008).
[3] R. Carminati and J.-J. Sáenz, Phys. Rev. Lett. **102**, 093902 (2009).
[4] G. Lerosey, J. de Rosny, A. Tourin and M. Fink, Science **315**, 1120 (2007).
[5] R. Carminati, R. Pierrat, J. de Rosny and M. Fink, Opt. Lett. **32**, 3107 (2007).

Threshold of a Random Laser with Cold Atoms

L.S. Froufe-Pérez

Instituto de Cicncia de Materiales de Madrid, CSIC.
Sor Juana Inés de la Cruz 3, Cantoblanco 28049, Spain.

luis.froufe@icmm.csic.es

Random lasing occurs when the optical feedback due to multiple scattering in a gain medium is strong enough so that gain in the sample volume overcomes losses through the surface. Since its theoretical prediction by Letokhov [1], great efforts have been made to experimentally demonstrate this effect in different kinds of systems, as well as to understand the fundamentals of random lasing. The broad interest of this topic is driven by potential applications and by its connections to the subject of Anderson localization.
State-of-the-art random lasers are usually based on condensed matter systems, and feedback is provided by a disordered scattering medium, while gain is provided by an active material lying in the host medium or inside the scatterers. In general, scattering and gain are related to different physical entities.

Another system that can be considered for achieving random lasing is a cold atomic vapor, using magneto-optical traps, where radiation trapping as well as lasing [2] have been demonstrated. One advantage is the ability to easily model the microscopic response of the system components, which can be extremely valuable to fully understand the physics of random lasers. However, in such a system, the ability to combine gain and multiple scattering at the same time is not obvious, as both should be provided by the same atoms.

In this work [3] we address this issue quantitatively. In particular, we show that the random laser threshold is described by a single critical parameter, the on-resonance optical thickness b_0. In the particular case of a gain mechanism based on a strongly-pumped two-level atom (Mollow gain), our model predicts a critical $b_0 \sim 300$. Such an optical thickness is achievable in current cold-atoms experiments. We have also determined the basic features of the emitted light above threshold, showing that the random laser emission should be measurable.

Acknowledgments

This work has been done in collaboration with the groups of Prof. R. Kaiser and Prof. R. Carminati in the framework of the project “Cold Atoms for Random Lasing” ANR-06-BLAN-0096.

References

[1] V. S. Letokhov, *Sov. Phys. JETP* **26**, 835 (1968).
[2] L. Hilico, C. Fabre, and E. Giacobino, *Europhys. Lett.* **18**, 685 (1992); W. Guerin, F. Michaud, and R. Kaiser, *Phys. Rev. Lett.* **101**, 093002 (2008).
[3] L. S. Froufe-Pérez, W. Guerin, Rémi Carminati, and R. Kaiser. *Phys. Rev. Lett.* **102**, 173903 (2009); W. Guerin, N. Mercadier, F. Michaud, D. Brivio, L. S. Froufe-Pérez, R. Carminati , V. Eremeev, A. Goetschy, S. E. Skipetrov y R. Kaiser. Acepted in *J. Opt. A: Pure Appl. Opt.* (2009).

Magnetoplasmonics: an overview on the fundamentals and applications

A. García-Martín, G. Armelles, A. Cebollada, J.M. García-Martín, M.U. González, E. Ferreiro, J.B. González-Díaz, J.F. Torrado, D. Martín-Becerra
Instituto de Microelectrónica de Madrid (IMM-CNM-CSIC),
Isaac newton 8, Tres Cantos, 28770 Madrid, Spain
antonio@imm.cnm.csic.es

Subwavelength composite materials constitute an interesting path towards the development of materials with "on demand" optical properties. We will present our latest results on systems composed of both noble and ferromagnetic metals, which we denote as magnetoplasmonic systems. While noble metals have intense and narrow plasmon resonances they lack magneto-optical (MO) activity at reasonable magnetic field intensities. On the other hand, ferromagnetic metals are MO active but their plasmon resonances are weak and broad. By combining both kinds of materials in smart structures we intend to obtain systems which simultaneously exhibit plasmon resonances and MO activity. Even more, we will show that in such systems it is possible both to enhance the magneto-optical activity of the system via surface plasmon excitation, and to modulate the plasmon properties via application of a magnetic field [1].

First we will concentrate on the effects of plasmon excitation on the MO response, starting from the analysis of Au/Co/Au nanodiscs [2] where it will be shown how the excitation of a localized surface plasmon (LSP) leads to an enhancement of the electromagnetic field within the MO active layer, which in turns produces an enhancement of the system MO activity (a factor of two at specific wavelengths). This latter effect has also been observed in pure Ni nanowires and membranes, characterized though by a much broader plasmon resonance [3]. The same influence of the LSP on the magneto-optical properties can be observed in systems where the constituents responsible for plasmon excitation and MO activity are spatially separated. This has been shown in structures formed by Au nanodiscs and Au/Co/Au continuous trilayers separated by layers of SiO_2[4]. Here the LSP excitation on the nanodiscs induces a redistribution of the electromagnetic field at the Co layer, and an enhanced magneto-optical activity occurs at those energies where the electromagnetic field in the magnetic layer is increased.

The same system will allow the analysis of the effect of the MO activity on the plasmon properties. We will show that the wavevector of the SPP is the physical magnitude which is modified upon application of a magnetic field in the transverse configuration [5]. In this case the application of a magnetic field in the transverse configuration affects the LSP and the surface plasmon polariton (SPP) excitation differently [6]. That modification can be used in a wide variety of scenarios. Here we will discuss its application in active nanointerferometry [7] and biosensing.

References

[1] G. Armelles, A. Cebollada, A. García-Martín, J. M. García-Martín, M. U. González, J. B. González-Díaz, E. Ferreiro and J. F. Torrado, J. Opt. A: Pure Appl. Opt. 11, 114023 (2009)
[2] J. B. González-Díaz, A. García-Martín, J. M. García-Martín, A. Cebollada, G. Armelles, B. Sepúlveda, Y. Alaverdyan, and M. Käll, Small 4, 202 (2008)
[3] J.B.González-Díaz, A. García-Martín, G. Armelles, D. Navas, M. Vázquez, K. Nielsch, R. Wehrspohn, and U. Gösele, Adv.Mater. 19, (2007) 2643; J.B.

González-Díaz, J. M. García-Martín, A. García-Martín, D. Navas, A. Asenjo, M. Vázquez, M. Hernández-Vélez, and G. Armelles, Appl. Phys. Lett. 94, 263101 (2009)

[4] G.Armelles, J. B. González-Díaz, A. García-Martín, J. M. García-Martín, A. Cebollada, M. U. González, S. Acimovic, J. Cesario, R. Quidant, and G. Badenes, Opt. Express 16, (2008) 16104

[5] J. B. González-Díaz, A. García-Martín, G. Armelles, J. M. García-Martín, C. Clavero, A. Cebollada, R. A. Lukaszew, J. R. Skuza, D. P. Kumah, and R. Clarke Phys. Rev. B 76, 153402 (2007); E. Ferreiro- Vila, J. B. Gonzalez- Díaz, R. Fermento, M. U. González, A. García- Martín, J. M. García- Martín, A. Cebollada, G. Armelles, D. Meneses-Rodríguez, and E. Muñoz Sandoval, Phys. Rev. B 80, 125132 (2009)

[6] J.F. Torrado, J.B. González-Díaz, M. U. González, A. García-Martín and G. Armelles, submitted (2009)

[7] V.V. Temnov, K. Nelson, G. Armelles, A. Cebollada, T. Thomay, A. Leitenstorfer and R. Bratschitsch, Optics Express 17, 8423 (2009), V. V. Temnov, G. Armelles, U. Woggon, D. Guzatov, A. Cebollada, A. Garcia-Martin, J. M. Garcia-Martin, T. Thomay, A. Leitenstorfer and R. Bratschitsch, submitted (2009)

Charge transport through bio-molecular wires in a solvent: Bridging molecular dynamics and model Hamiltonian approaches

Rafael Gutierrez

Institute for Materials Science, Dresden University of Technology
01062 Dresden, Germany

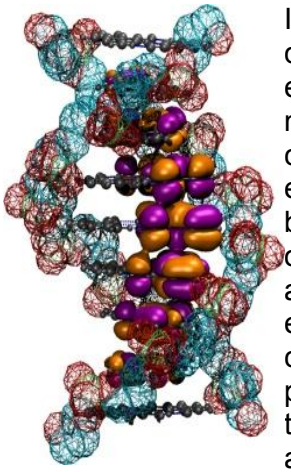

I will present a hybrid method based on a combination of quantum/classical molecular dynamics (MD) simulations and a mod el Hamiltonian approach to describe charge transport through bio-molecular wires with variable lengths in presence of a solvent. The core of our approach consists in a mapping of the bio-molecular electronic structure, as obtained from density-functional based tight-binding calculations of molecular structures along MD trajectories, onto a low dimensional model Hamiltonian including the coupling to a dissipative bosonic environment. The latter encodes fluctuation effects arising from the solvent and from the molecular conformational dynamics. We apply this approach to the case of pG-pC and pA-pT DNA oligomers as paradigmatic cases and show that the DNA conformational fluctuations are essential in determining and supporting charge transport.

References

[1] R. Gutierrez, R. Caetano, P.B. Woiczikowski, T. Kubar, M. Elstner, and G. Cuniberti, Phys Rev. Lett. 102, 208102 (2009).

[2] P. B. Woiczikowski, T. Kubar, R. Gutierrez, R. Caetano, G. Cuniberti, and M. Elstner, J. Chem. Phys. 130, 215104 (2009).

IR and THz nanoscopy for characterizing electronic and photonic nanostructures

Rainer Hillenbrand

Nanooptics Laboratory, CIC nanoGUNE, 20018 Donostia - San Sebastian, Spain
r.hillenbrand@nanogune.eu

We demonstrate nanoscale resolved IR and THz imaging by recording the elastically scattered light from the laser-illuminated tip of an atomic force microscope tip (scattering-type near-field optical microscopy, s-SNOM).

Using metal-coated AFM tips, the strong field concentration at the tip apex probes the local dielectric properties of a sample, allowing for the simultaneous recognition of materials and free-carrier concentration in semiconductor nanodevices [1] (Fig. 1) and nanowires. Quantitative free-carrier mapping is enabled by near-field plasmon-polariton spectroscopy, which can be also applied to study strain-induced changes of carrier concentration and mobility [2]. Nanoscale imaging of strain and nanocracks in ceramics can be achieved by near-field infrared phonon-polariton spectroscopy [2].

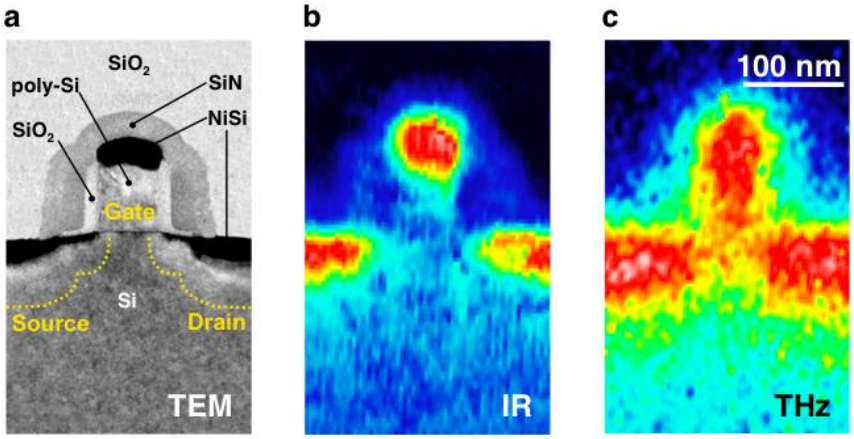

Figure 1: *Nanoscale resolved images of a single transistor of the 65 nm-technology. (a) TEM image. (b) Near-field IR image taken at about 11 µm wavelength. (c) THz near-field image taken at 118 µm wavelength. In contrast to TEM and IR, the THz image reveals the distribution of mobile carriers below the metallic NiSi contacts.*

Employing dielectric tips, s-SNOM also enables the mapping of near-field patterns generated by plasmonic nanoantennas [3]. The tip essentially scatters the near fields at the sample surface. Recently, we applied s-SNOM to monitor the evolution of the near-field oscillations of gap antennas progressively loaded with metallic bridges of varying size. Our results provide direct experimental evidence that the local near-field amplitude and phase can be controlled by antenna loading, which is in excellent agreement with numerical calculations [4].

References

[1] A. Huber, *et al.*, *Nano Lett.* **8**, 3766 (2008)
[2] A. Huber, *et al.*, *Nature Nanotech*. **4**, 153 (2009)
[3] R. Hillenbrand *et al.*, *Appl. Phys. Lett.* **83**, 368 (2003)
[4] M. Schnell, *et al.*, *Nature Photon*. **3**, 287 (2009)

Carbon Nanotube Spintronics

Luis E. Hueso

CIC nanoGUNE, San Sebastian, Spain and
IKERBASQUE, Basque Foundation for Science, Bilbao, Spain

l.hueso@nanogune.eu

Spintronics is a branch of electronics that aims to take full advantage of, not only the charge, but also the spin of the electron. Spintronic applications are commercially available in the spin valves of disc-drive read heads and in magnetic random access memories. These devices exploit the spin coherent transport of the electron at small distances (in the order of magnitude of 1 nm), but there is certainly also much interest in spin coherent transport and manipulation over longer distances (larger than 100 nm), both in metals and semiconductors. However, the transformation of spin information into large electrical signals is limited by spin relaxation such that the magnetoresistive signals are below 1% [1].
However, promising results have being obtained when the non-magnetic channel is a carbon-based material, such as a carbon nanotube, graphene or an organic semiconductor.
In this seminar, I will present large magnetoresistance effects (70% at 5 K) in devices where a multiwall carbon nanotube spans between epitaxial electrodes of the highly spin polarized manganite $La_{0.7}Sr_{0.3}MnO_3$ (LSMO). This improved result arises from several factors: 1) because the spin lifetime in nanotubes is long due the small spin-orbit coupling of carbon, 2) because the high nanotube Fermi velocity permits the carrier dwell time to not significantly exceed this spin lifetime, and 3) because the interfacial barrier between the nanotube and the manganite is of an appropriate height [2,3]. These results could open a viable way of converting spin information into electrical signals.
During the talk, I will also put these results in the wider context of the research of spintronics with carbon-based materials, highlighting their potentialities and current unresolved issues.

References

[1] A. Fert, J.M. George, H. Jaffres, and R. Mattana, IEEE Trans. Electron. Devices 54, 921 (2007)
[2] L.E. Hueso, G. Burnell, J.L Prieto, L Granja, D.-J. Kang, M. Chhowalla, S.N. Cha, J.E. Jang, G.A.J. Amaratunga, and N.D. Mathur, Appl. Phys. Lett. 88, 083120 (2006)
[3] L.E. Hueso, M.A. Pruneda, V. Ferrari, G. Burnell, J. Valdes, B. Simons, P.B. Littlewood, A. Fert, and N.D. Mathur, Nature 445, 410 (2007)

Electronic, Optical and Transport properties of semiconducting nanowires : Theory and modeling

Y. M. Niquet[1], M. Persson[1], A. Lherbier[1,2], D. Camacho[1], F. Triozon[3], and S. Roche[4],
[(1)] CEA/INAC/SP2M/L_Sim, [(2)] CNRS/LTM (UMR CNRS 5129), [(3)] CEA LETI-MINATEC,
[(4)] CEA/INAC/SPSMS/GT, 17 rue des Martyrs, 38054 Grenoble Cedex 9, France.

M. Diarra, C. Delerue and G. Allan,
IEMN Dept ISEN (UMR CNRS 8520), 41 boulevard Vauban, F-59046 Lille Cedex, France.

Semiconducting nanowires are promising candidates for nano and optoelectronics applications. They indeed show original optical and transport properties, which are however not yet fully understood. In this context, theory and modeling can sched some light onto the physics of these nanostructures, and help understand their behavior, especially in the < 20 nm diameter range where quantum and dielectric confinement have significant effects. In this talk, we review our latest results on the optical and transport properties of semiconducting nanowires. We use tight-binding methods for the electronic structure and quantum Kubo-Greenwood or Green function techniques for transport calculations. We discuss, in particular, the transport properties of ultimate silicon nanowires (d < 5 nm), and their dependence on the growth direction. The electronic properties (electron and hole effective masses, valley degeneracies and splittings...) of such nanowires indeed strongly depend on their orientation due to the anisotropy of the band structure of silicon, which shows up on the mobility in the quantum regime where only one or a few subbands are occupied. We focus on surface roughness and on neutral or ionized dopant impurities as examples, taking into account the complex dielectric environement (high-k oxydes and/or wrap-around gates) encountered in actual devices. We also discuss the effects of strains on the electronic and optical properties of axial and core-shell nanowire heterostructures. We show, in particular, that the residual strains can significantly lower the height of tunnel barriers in nanowires, and that the interplay between strains, lateral and longitudinal confinement can change the polarization of the light emitted by quantum dots embedded in nanowires. We compare the respective properties of wurtzite and zinc-blende nanowires. This work was partly supported by the EU project NODE and the French ANR Quantamonde.

Transport properties of carbon nanotube links between graphene layers

F. D. Novaes[1], R. Rurali[1] and P. Ordejón[2]

[1]Instituto de Ciencia de Materiales de Barcelona - CSIC, Campus de la UAB, 08193 Bellaterra, Barcelona, Spain
[2]Centro de Investigación en Nanociencia y Nanotecnología - CIN2 (CSIC-ICN), Campus de la UAB, 08193 Bellaterra, Barcelona, Spain

The study of electronic transport both in graphene and in carbon nanotubes has attracted a great deal of work, due to the interesting fundamental phenomena that these materials display and to the promise of outstanding applications in nanoelectronics [1,2]. The two- and one-dimensional character of the two materials, respectively, confer them with sharply different electronic transport properties, and therefore different potential applications are envisioned.

In this work, we have considered the possibility of future devices that may use combinations of graphene layers and carbon nanotubes for electronic applications. For instance, nanotubes might be used to transmit electronic signals between two graphene-based devices, in the same way as copper wires do between traditional silicon-based transistors [3].

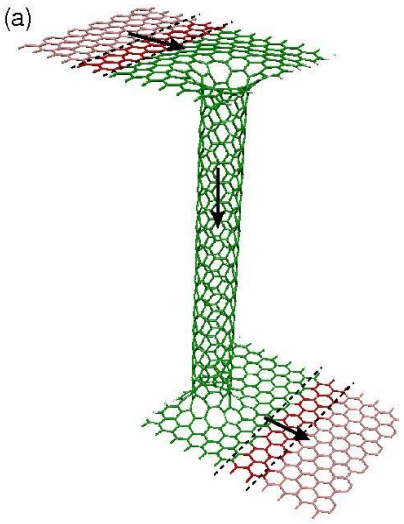

Figure 1: *Scheme of the setup used in the transport calculations: two semi-infinite graphene sheets are connected by a finite length nanotube. The link is covalent, maintaining the sp^2 coordination.*

We present first-principles studies of the transport properties of a system consisting on two graphene sheets connected by a carbon nanotube. We consider different nanotubes with different chiralities and lengths, and also different types of connections between the tube and the sheet. We compute the ballistic transport between the two sheets through the nanotube, and show that the behavior of the conductance is qualitatively different for metallic and semiconducting nanotubes. We also show how the conductance depends on the link between the nanotube and the graphene sheet.

Figure 1 shows a scheme of the geometry used in our calculations. We have done calculations with both metallic armchair (4,4), and semiconducting zigzag (8,0) nanotubes, and with two different structures of the link between graphene and nanotube [4].

In Figure 2 we show the dependence of the conductance (for a voltage of 0.6 V between both graphene sheets), as a function of nanotube length, for the (4,4) and (8,0) tubes. For the metallic tubes, the conductance does not decrease with increasing the nanotube length, indicating transport by extended states as expected for a metallic system. For the semiconducting tubes, however, the conductance decreases exponentially with nanotube length, indicating transport by tunneling.

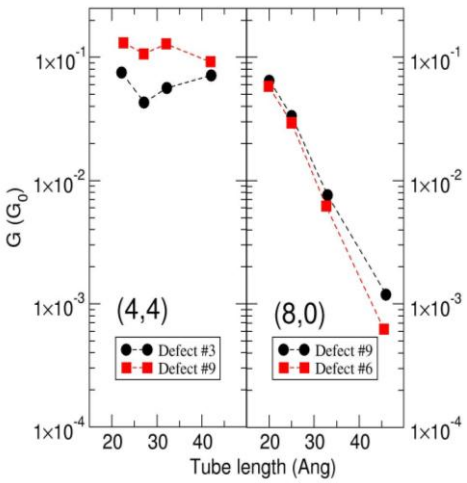

Figure 2: *Dependence of the conductance (computed for a 0.6 V bias voltage) for the metallic (4,4) and the semiconducting (8,0) nanotubes.*

References

[1] Charlier, J.-C.; Blase, X.; Roche, S. *Rev. Mod. Phys.* **2007**, *79*, 677.
[2] Neto, A. H. C.; Guinea, F.; Peres, N.M. R.; Novoselov,K. S.; Geim, A. K. *Reviews of Modern Physics* **2009**, *81*, 109–162.
[3] Ferry, D. K. *Science* **2008**, *319*, 579–580.
[4] Baowan, D.; Cox, B. J.; Hill, J. M. *Carbon* **2007**, *45*, 2972–2980.

Applying Magnetic Field to Carbon based Low Dimensional Materials: from Aharonov Bohm Effects to the Landau Level formation

Stephan Roche

CIN2 (ICN-CSIC), Campus UAB, Bellaterra (Barcelona), Spain
CEA, INAC, SP2M, L_sim, Grenoble, France
http://inac.cea.fr/Pisp/22/stephan.roche.html

In this talk, we will discuss several magnetic-field dependent transport phenomena in carbon nanotubes based materials [1]. First on will review the Aharonov-Bohm phenomenon in weakly disordered metallic nanotubes, when an external magnetic field is applied parallel to the tube axis. The position of the Fermi level and the nature of underlying disorde r will be shown to critically affect the corresponding magnetofingerprints, in agreement with experimental observations. Calculations are performed within a simple tight-binding model, and the effect of the magnetic field is modelled by the Peierls substitution. The presence of impurity-induced quasibound states (as appearing in chemically doped carbon nanotubes) will be also shown to yield switching from negative to positive magnetoresistance [2]. In a second part, the occurence of Landau levels for magnetic applied perpendicular to the nanotube axis will be discussed in the light of recent experiments [3].

References

[1] J.C. Charlier, X. Blase and Stephan Roche, *Electronic and Transport in Carbon Nanotubes*, Review of Modern Physics 79, 677 (2007)

[2] S. Roche, F. Triozon, A. Rubio, D. Mayou, *Conduction mechanisms in multiwalled carbon nanotubes*, Physical Review B (RC) 64, 121401(R) (2001). S. Latil, F. Triozon, S. Roche, *Anomalous Magnetotransport in Chemically Doped Carbon Nanotubes,* Physical Review Letters 95, 126802 (2005). G. Fedorov, A. Tselev, D. Jimenez, S. Latil, N. Kalugin, P. barbara, and S. Roche, *Exploring the Magnetic induced Field Effect Efficiency in Carbon Nanotube Based Devices*, Nano Lett. 7 (4), 960 (2007)

[3] B. Raquet, R. Avriller, B. Lassagne, S. Nanot, W. Escoffier, J.-M. Broto, S. Roche, *Landau Level Formation in Carbon Nanotubes-Based Electronic Fabry-Perot Resonators,* Physical Review Letters 101, 046803 (2008).

Nanoparticle Dynamics in Non-Conservative Optical Vortex Fields

S. Albaladejo[1], I. Zapata[2], M. I. Marqués[1], M. Laroche[3], J.M. Parrondo[4], F. Scheffold[5], F. Sols[2] and J.J. Sáenz[1]

[1]*Moving Light and Electrons (Mole) Group, Univ. Autónoma de Madrid, Spain.*
[2]*Dpto. Física de Materiales, Universidad Complutense de Madrid, Spain.*
[3]*Institut d'Optique, CNRS, Université Paris-Sud, France.*
[4]*Dpto. Física Atómica y Molecular, Universidad Complutense de Madrid, Spain.*
[5]*Department of Physics, University of Fribourg, Switzerland*

Light forces on small (Rayleigh) particles are usually described as the sum of two terms: the dipolar or gradient force and the scattering or radiation pressure force. The scattering force is traditionally considered proportional to the Poynting vector, which gives the direction and magnitude of the momentum flow. However, as we will show, when the light field has a non-uniform spatial distribution of spin angular momentum, an additional scattering force arises as a reaction of the particle against the rotation of the spin. This non-conservative force term is proportional to the curl of the spin angular momentum of the light field [1]. We will illustrate the relevance of the spin force in the particular simple case of a 2D field geometry arising in the intersection region of two standing waves [2].

We will also discuss the peculiar particle dynamics in the non-conservative force field of an optical vortex lattice [3]. Radiation pressure in the whirllight field (arising in the intersection region of two crossed optical standing waves [2]) plays an active role spinning the particles out of the whirls sites leading to a giant acceleration of free diffusion. Interestingly, we show that a simple combination of null-average conservative and nonconservative steady forces can rectify the flow of damped particles. We propose a "deterministic ratchet" stemming from purely stationary forces [4] that represents a novel concept in dynamics with considerable potential for fundamental and practical implications.

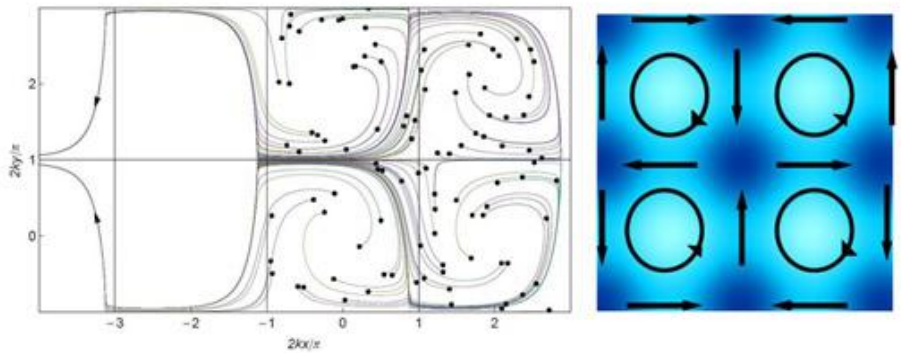

References

[1] S. Albaladejo, M. Laroche, M. Marques, J.J. Saenz, Phys.Rev.Lett. 102 , 113602 (2009)
[2] A. Hemmerich, T.W. Hänsch, Phys. Rev. Lett. 68, 1492 (1992).
[3] S. Albaladejo, M.I. Marques, F. Scheffold, J.J. Saenz, Nano Letters, 9, 3527 (2009).
[4] I. Zapata, S. Albaladejo, J.M. Parrondo, J.J. Saenz, F. Sols, PRL, 103, 130601 (2009)

Tilt angle dependence of electronic transport in molecular junctions of self-assembled alkanethiols

T. Frederiksen[1,2], C. Munuera[4], C. Ocal[4], M. Brandbyge[5], M. Paulsson[6], A. Arnau[1,2,3] and D. Sánchez-Portal[1,2]

[1] Donostia International Physics Center (DIPC), Paseo Manuel de Lardizabal 4, San Sebastián 20018, Spain and CIC nanoGUNE Consolider, Av. Tolosa 76, San Sebastián 20018, Spain

[2] Unidad de Física de Materiales, Centro Mixto CSIC-UPV, Apdo. 1072, San Sebastián 20080, Spain

[3] Departamento de Física de Materiales UPV/EHU, Facultad de Química, Apdo. 1072, San Sebastián 20080, Spain

[4]Institut de Ciencia de Materials de Barcelona, CSIC, Bellaterra 08193, Spain

[5]DTU Nanotech, NanoDTU, Technical University of Denmark, 2800 Lyngby, Denmark

[6]School of Pure and Applied Natural Sciences, UniVersity of Kalmar, 391 82 Kalmar, Sweden

Measurements done using conductive scanning force microscopy under low load conditions permit to obtain reliable tilt angle and molecular length dependences of the low bias conductance through the alkanethiol molecular layers [1]. We use several well-characterized self-assembled structures of alkanethiol molecules on Au(111) where molecules present different angles with respect to the surface normal. The observed tilt-angle dependence of the conductance is stronger for the longer molecular chains (see the Table 1 below) and, therefore, would suggest the importance of intermolecular (through space) tunneling pathways.

tilt angle	***R*** **(C12)**	***R*** **(C16)**	***R*** **(C18)**
30	$1.3x10^{2}$	$2.5x10^{3}$	$2.08x10^{4}$
50	$6.5x10^{1}$	$3.3x10^{2}$	$1.7x10^{3}$
ratio	2.0	7.6	12.2

Table 1: *Measured Junction Resistances R (in GΩ) as a function of Alkane Backbone Length and Tilt Angle (in deg)*

To model this system we have performed first-principles calculations of the transport through monolayers of alkanedithiols between two Au(111) electrodes [1]. The tilt angle dependence of the calculated conductance is similar to that observed experimentally (see the accompanying Figures). We use our theoretical results to analyze in detail the different mechanisms contributing to the observed behavior. We find two main contributions: i) a contribution from intermolecular tunneling as previously suggested in the literature and, ii) a previously overlooked tilt dependent molecular gate effect. In this second mechanism, the position of the molecular HOMO respect to the Fermi level of the metallic substrate changes following the modification of the surface dipole. The surface dipole has a simple dependence on the tilt angle that can be associated with the different orientiation of the S-C bond of the molecule respect to the surface normal.

References

[1] Th. Frederiksen *et al.*, ACS Nano **3**, 2073–2080 (2009)

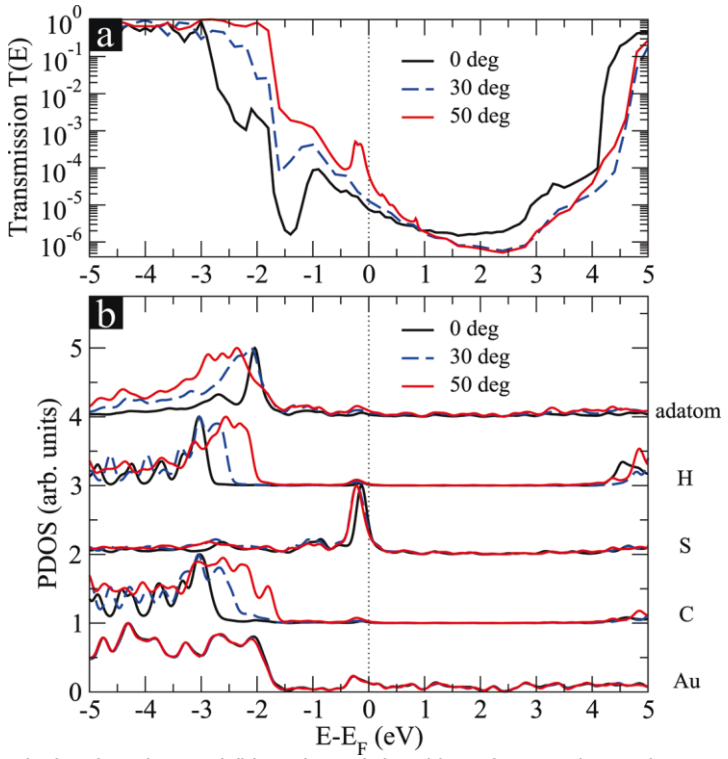

Figure 1: *(a) Transmission function and (b) projected densities of states (PDOS) onto different atoms as a function of electron energy for C12 at three different nominal tilt angles.*

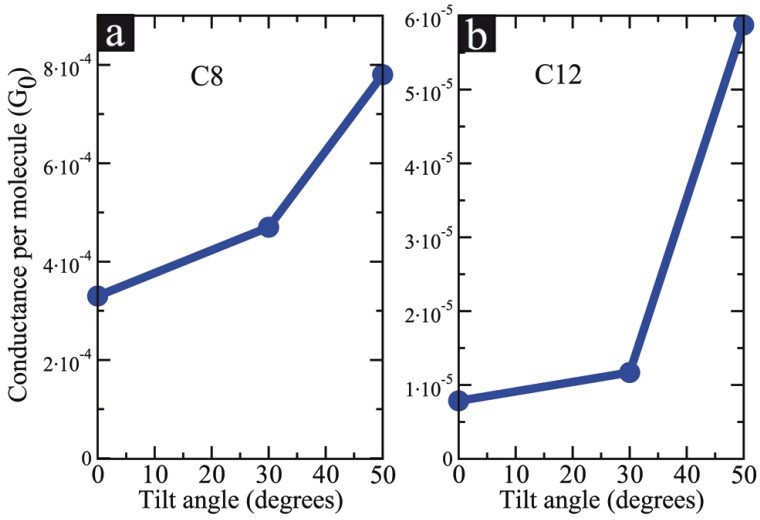

Figure 2: *Theoretically computed conductance per molecule for C8 and C12 for different nominal tilt angles.*

Controlling photon emitters on nanometer and femtosecond scale

Niek F. van Hulst[#]

Daan Brinks, Tim Taminiau, Alberto Gonzalez-Curto, Richard Hildner, Fernando Stefani, Marta Castro, Florian Kulzer

ICFO – Institute of Photonic Sciences, 08860 Castelldefels - Barcelona, Spain.
[#]*ICREA – Institució Catalana de Recerca i Estudis Avançats, 08015 Barcelona, Spain.*
Niek.vanHulst@ICFO.es *www.ICFO.es*

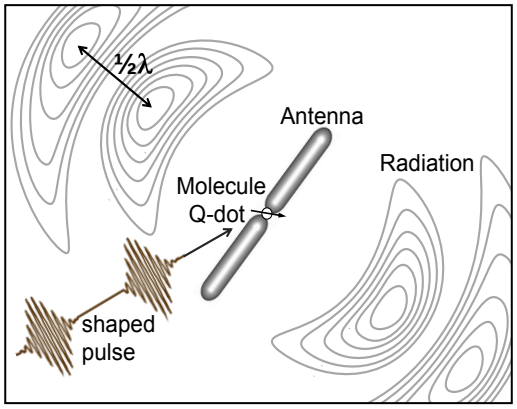

Figure 1: *Nanoscale control of single photon emission; A single molecule or quantum dot interacts with free optical radiation via a nano-optical antenna. In close proximity to the resonant nano-antenna the emitter exhibits enhanced excitation and decay rates and redirected emission [2]. Excitation by phase shaped fs pulses allows to control the excitation path.*

Advances in both detection of single photon emitters and fabrication of nanostructures now allow the exploration of light in and around nanostructures, single molecules, molecular complexes, etc. Indeed by proper control on the nm-scale sub-wavelength strong light fields are being created and detected. In the nanoworld single molecules or nanoparticles are the ultimate detectors of both local optical fields and interaction with the local environment. Here we focus on the control of single molecules using resonant nano-antenna and phase shaped fs pulses.
We show how both excitation and emission of individual molecules is controlled by coupling to resonant optical nano-antennas. The molecule probes the local antenna field and here we show optical fields of a resonant monopole antenna, spatially localized within 25 nm [1]. Next the enhancement of the radiative and excitation rates is treated, particularly how the angular emission of the coupled system is highly directed, as the dominant antenna mode determines the angular emission. Thus arbitrary control over the main direction of emission is obtained, regardless of the orientation of the emitter [2]. A nano-Yagi-Uda antenna is discussed affording enhanced rates, strong unidirectional emission and, in reciprocity, efficient nano-focusing, making such antennas a promising candidate for compact easy-to-address planar sensors at the single molecule level [3]. By excitation of the coupled system with phase controlled fs pulses we control on fs time scale the build-up of the antenna mode and thus the positions of field enhancement along the antenna.
The combined spatio-temporal control is promising for controlled single photon sources, light harvesting systems, efficient bio-sensors and optical imaging with 10 nm resolution.

References

[1] Taminiau, T. H., Moerland, R. J., Segerink, F. B., Kuipers, L. & van Hulst, N. F. □/4 resonance of an optical monopole antenna probed by single molecule fluorescence. *Nano Lett.* 7, 28–33 (2007).
[2] Taminiau, T.H., Stefani, F.D., Segerink, F.B. and van Hulst, N.F., Optical antennas direct single molecule emission, *Nature Photonics* **2**, 234 (2008).
[3] Taminiau, T.H., Stefani, F.D. and van Hulst, N.F., Enhanced directional excitation and emission of single emitters by a nano-optical Yagi-Uda antenna, *Opt. Express* 16 10858 (2008).

Abstracts – Posters

Alphabetical Order

School 1 (NanoOptics and NanoPhotonics)
&
School 2 (Modeling)

Explicit computation of Bohm velocity for N-electrons in open quantum systems

A. Alarcón , X.Cartoixà and X.Oriols
Departament d'Enginyeria Electrònica,
Universitat Autònoma de Barcelona, 08193, Bellaterra, Spain
Contact E-mail: Alfonso.Alarcon@uab.es

From a computational point of view, the direct solution of the many-particle Schrödinger equation is inaccessible for more than very few electrons. This issue is at the heart of almost all the unsolved problems in quantum transport. Recently, a novel many-particle quantum transport formalism using Bohm trajectories has been presented for dealing with Coulomb and exchange interaction among electrons [1]. We discuss the computational burden associated with the explicit consideration of the electron spin in the previous formalism [1]. In particular, we have provided a numerical justification that shows the viability of previous formalism for studying systems with a large (N~100) number of electrons. We consider a system of *N* electrons described by a many-particle wave-function $\Psi(\vec{r}_1,\vec{r}_2,\vec{r}_3..\uparrow_1,\downarrow_2,\downarrow_3..)$ with $\vec{r}_i$ the electron position and $\uparrow_i$ / $\downarrow_i$ its (up/down) spin. We use an uncoupled spin-base which is adequate for (non-conservative spin) open systems. In the previous formalism [1], the Bohm velocity of each electron has to be computed directly from the many-particle wave-function. In addition, the explicit evaluation of *N*!·*N*! products of permutations for the computation of the many-particle system is intractable for more than very few electrons because of computational limitations (note that $8!^2 = 40320^2$). The previous computational limitation is overcome by computing the many-particle Bohm velocity with the assumption that the many-particle wavefunction can be separated into a product of spin-up (↑) and spin-down (↓) many-particle wave functions:

$$\Psi(\vec{r}_1,\vec{r}_2,\vec{r}_3..\uparrow_1,\downarrow_2,\downarrow_3..)\approx\Psi(\vec{r}_1,\vec{r}_4,..\uparrow_1,\uparrow_4..)\cdot\Psi(\vec{r}_2,\vec{r}_3..\downarrow_2,\downarrow_3..). \quad (1)$$

Then, the numerical difficulties in the computation of the many-particle Bohm velocity disappear because it can be computed from a complex matrix (Slater) determinant. We have defined the parameter *d* as a normalized (i.e. without units) phase-space distance [2] between electron 1 and the others (see insets in all Figures). Also, we have chosen arbitrary initial Gaussians wave-packets. In order to numerically verify the correctness of our assumption, we compute the Bohm velocity associated to electron 1 in three different (exchange-interacting) situations: independent electron, exact computation and computational approximation showed in the schemes of Figure 1, Figure 2, and Figure 3 respectively. In detail, in Figure 1, we show the Bohm velocity (with an approximate value of $6x10^4$ m/s) for one independent (spin-up) electron. In Figure 2, we plot the exact computation of Bohm velocity for a system of 5 electrons studying the electron 1 when other 4 exchange-interacting electrons are present. In this case, when we decrease the distance *d* among electrons, the Bohm velocity becomes very different from Figure 1 as a consequence of the Pauli (Exclusion) Principle. In Figure 3, we consider a computational approximation for the system with 5 electrons studying only the 3 spin-up electrons of Figure 2. The strong resemblance between the Bohm velocities of Figures 2 and 3 for the different values of *d* provides a numerical justification of expression (1) for the computation of many-particle Bohm velocities. The same result is obtained for many other spin schemes. The differences between the two schemes presented in Figures 2 and 3 are explained in Figure 4. For a particular position (X=150nm) of Figures 2 and 3 we plot the Bohm velocity in function distance *d* among electrons for these two different electron scenarios. We observe in Figure 4 two different zones: zone with for *small d* and zone for *large d* (circle dashed lines). For justify the differences between the exact computation and the computational

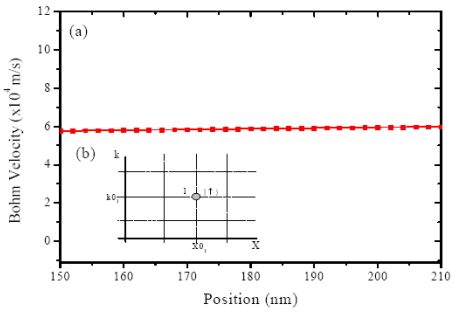

Figure 1: *(a) Bohm velocity for an independent electron. (b) Schematic representation of the system for an electron where we indicate the central value of the X_0 and wave-vector K_0.*

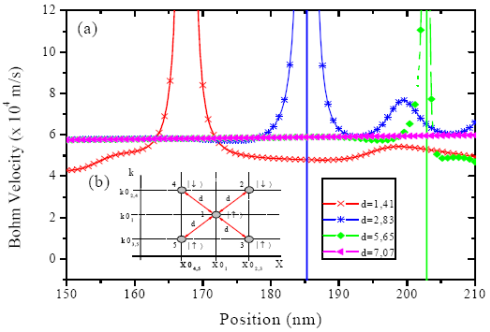

Figure 2: *(a) Bohm velocities for 1-electron using different values of d for a system of 5 electrons (3 spin-up and 2 spin-down). (b) In this scheme we indicate the central value of the X_0 and wave-vector K_0 of these electrons.*

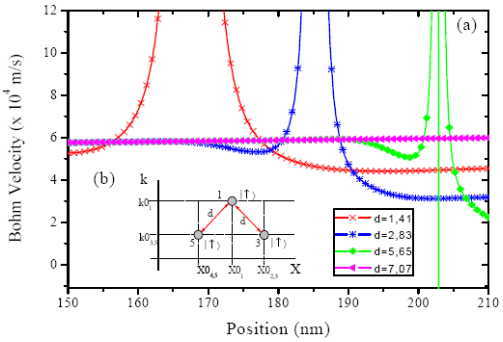

Figure 3: *Bohm velocities for 1-electron using different values of d for a system of 3 electrons (spin-up). (b) In this scheme we indicate the central value of the X_0 and wave-vector K_0 of these electrons.*

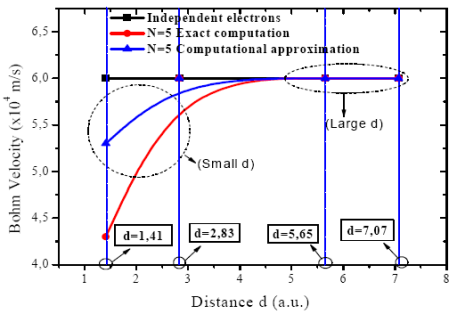

Figure 4: *For a particular position (X=150nm) of Bohm velocity of Figure 2 and Figure 3. We plot the Bohm velocity in function distance d among electrons for two different electron scenarios.*

approximation that we observe for *small d* inside Figure 4 is necessary to treat with detail the total norm that we use for compute the Bohm velocity of particle 1. In detail, the total norm is divided in two parts: principal contribution and spurious contribution. In the particular scenario for *small d* we find a significant spurious contribution. Or contrary, in the particular scenario for *large d* the spurious contribution is almost zero.

In conclusion, we present an approximation expression (1) to study the many-particle Schrödinger equation in spin-dependent systems. In order to overcome the computational limitations associates to these systems, we propose that a many particle wave functions can be separated in a product of spin up and spin down many-particle wave functions. To verify our assumption we present a numerical justification computing the Bohm velocity in three different (exchange–interacting) schemes. The practical viability of our proposal can be used for study systems of large (N~100) number of electrons using Slater determinants. Also, this study has significant implications in electron quantum transport with Coulomb and exchange interactions among electrons. In next future we will treat with time-dependent Schrödinger equations in terms of Bohm trajectories. This approach will apply for the computation of the average current or its fluctuations [3] in zero or high frequency [4] quantum scenarios.

This work was supported through Spanish MEC project MICINN TEC2009-06986.

References

[1] X.Oriols, Physical Review Letters, 98, 066803 (2007).
[2] X.Oriols, Nanotechnology 15, S167- S175 (2004).
[3] G. Albareda, J.Suñe, X. Oriols, Phys. Rev. B 79, 075315 (2009).
[4] A.Alarcon, X.Oriols, J. Stat. Mech, 2009 (P01051) (2009).

Coulomb-correlations in the electric power of nanoscale open systems

G.Albareda and X.Oriols
Departament d'Enginyeria Electrònica, Universitat Autònoma de Barcelona, 08193 Bellaterra, Spain
guillem.albareda@uab.cat

Due to computational limitations, one necessary strategy to study nanoscale structures is to reduce, as much as possible, the simulated degrees of freedom. This procedure is always traumatic because, in general, a subcomponent of the whole system cannot be described independently of the rest (See Figure 1). The openness of classical and quantum systems has been studied extensively in the literature, but few works are devoted to discuss its effect on the computation of electric power. Here, we provide a novel expression for accurate estimation of the electric power in nanoscale open systems using a many-particle electron transport formalism that goes beyond the standard "mean field" approximation [1]. Surprisingly, we show that the usual expression of the electric power, as the product of the (time-averaged) current $\langle I \rangle_T$ and the applied voltage ΔV, is not correct in nanoscale systems.

In order to provide a common classical and quantum language for our argumentation, we formulate the problem in terms of the de Broglie–Bohm approach of quantum mechanics for an open system of non-relativistic (spinless) Coulomb-interacting electrons [1,2]. Then, it can be shown that the mean electric power, P, for the *N(t)* electrons inside the open system (see Figure 1b) is:

$$P = \left\langle \sum_{i=1}^{N(t)} q\vec{v}_i(t)\vec{E}_i(\vec{r}_i(t)) \right\rangle_B = \lim_{T\to\infty} \frac{1}{T} \sum_{i=1}^{M(T)} q(K_i(L) - K_i(0)) \qquad (1)$$

where $\vec{v}_i(t)$ is the (Bohm) velocity of the *i* electron, $q\vec{E}_i(t)$ is the electrostatic force made by the rest of electrons of the whole (closed) system on it, and $K_i(L)$ and $K_i(0)$ are its (Bohm) kinetic energies at the final and initial positions respectively. Here, $\langle ... \rangle_B$ is the de Broglie-Bohm averaging that can be converted into time averaging $\langle ... \rangle_T$ under standard ergodic argumentations. After some straightforward development, the final value of the mean electric power P of expression (1) can be written as:

$$P = \langle I \rangle_T \cdot \Delta V - \left\langle \frac{q}{2} \sum_{i=1}^{N(t)} \sum_{\substack{j=1 \\ j\neq i}}^{N(t)} (\vec{v}_j - \vec{v}_i) \cdot \frac{(\vec{r}_i - \vec{r}_j)}{4\pi\varepsilon |\vec{r}_i - \vec{r}_j|^3} \right\rangle_T \qquad (2)$$

where $W_i(\vec{r}_1,..,\vec{r}_j,..,\vec{r}_i(t),..,\vec{r}_M)$ is the *i-th* electrostatic potential defined in Ref. [1] that depends on the *M* electrons present in the close (whole) system (see Figure 1a) and $\vec{R}_i(\vec{r}_1(t),..,\vec{r}_j(t),..,\vec{r}_{i-1}(t),..,\vec{r}_{i+1}(t),..,\vec{r}_M(t))$. The first term on the right side of (2) is the standard $\langle I \rangle_T \cdot \Delta V$ power expression, while the second term represents the effects of the many-particle coulomb correlations on the electric power.

In order to show the relevance of the many-particle power correlations, we have simulated a nanoscale resistance using, both, a standard single-particle semiconductor

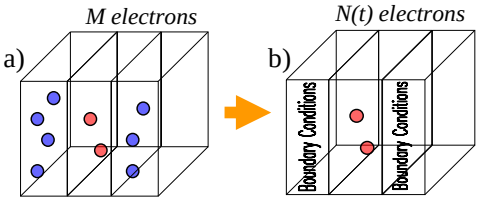

Figure 1: *Schematic representation of the electrons in an electron device. a) A closed (whole) system of M electrons in the active region and the reservoirs and b) the open system of N(t) electrons in the active region.*

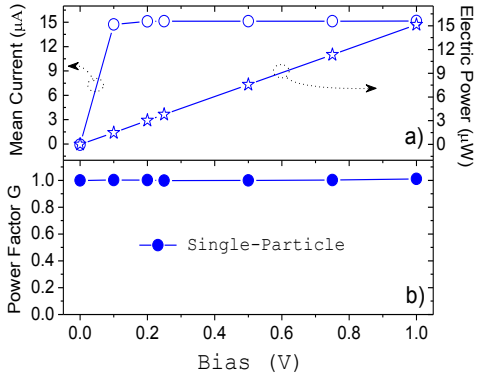

Figure 2: *a) Average current, electric power, and b) correlation power factor, G, defined in the text as a function of bias. Electron transport is computed from a single-particle approach*

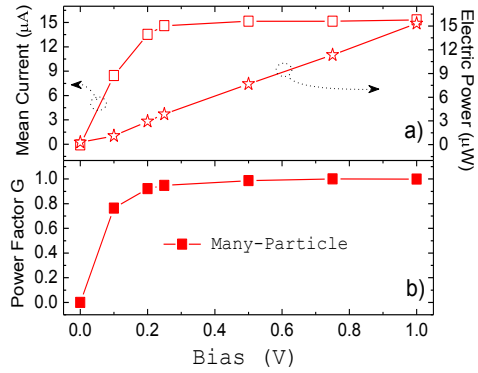

Figure 3: *a) Average current, electric power, and b) correlation power factor, G, defined in the text as a function of bias. Electron transport is computed from the many-particle approach described in [1].*

Monte Carlo simulator and a many-particle electron transport approach explained in Ref. [1]. In Figure 2a, we have represented the current-voltage characteristic for a nanoscale resistance using a single-particle (i.e. time-independent electric-field) electron transport approach. We define the correlation power factor as the following (dimensionless) parameter, $G = (\langle I \rangle T \cdot \Delta V)/P$. As expected, the value of G reduces to unit, i.e. $P \approx \langle I \rangle_T \cdot \Delta V$, indicating that many-particle Coulomb-interaction effects in the power computation are not accessible with single-particle electron transport simulations. On the contrary, when the many-particle electron transport formalism explained in Ref. [1] is used, then, the relevance of correlations in the average power becomes evident (at low bias) in the correlation power factor G depicted in Figure 3b.

The physical explanation of our "unexpected" many-particle corrections on the electric power is that the computation of power in numerical simulators has to account only for the (non-conservative) energy associated to the *N(t)* electrons inside the open system rather than the (conservative) energy of the M electrons inside the whole system (see Figure 1).

References

[1] G. Albareda, J. Suñé and X. Oriols, Physical Review B, **79** (2009) 075315.
[2] X. Oriols, Physical Review Letters, **98** (2007) 066803.

Coupling of light into nanowire arrays and subsequent absorption

Nicklas Anttu[1, a,] and Hongqi Xu[1,b]*
[1]Division of Solid State Physics/The Nanometer Structure Consortium, Lund University, P O Box 118, S-221 00 Lund, Sweden
[a]Nicklas.Anttu@ftf.lth.se , [b]Hongqi.Xu@ftf.lth.se
**Corresponding author*

Keywords: Light, absorption, scattering, subwavelength, semiconductor, nanowire, periodic array, photovoltaics, solar cells

In this work we report on a theoretical study of the coupling of light into an array of III-V semiconductor nanowires and subsequent absorption in the array. The response to incident light was modeled with the Maxwell equations that were solved with our novel scattering matrix method[1]. We found the absorption in the array to depend on the material, diameter and length of the nanowires, as well as the period of the array. Nanowires of a length of just 2 μm were able, after an appropriate choice for the other parameters, to absorb above 90% of the incident energy of both TE and TM polarized incident light, with photon energy more than 5% above the band gap, for incidence angles up to 60 degrees. This high total absorption arises from a good single interface coupling of light into the nanowire array at the interface between air and the array and absorption inside the array before the light reaches the interface between the nanowires and the substrate. We found that for a given photon energy there exists a critical nanowire diameter above which a dramatic increase in the absorption occurs. The critical diameter decreases for increasing photon energies. Simple models based on an effective refractive index for the array, calculated from the filling factor of the nanowires, could not reproduce this diameter dependence, highlighting the importance of using full electromagnetic simulations. The critical diameter can be explained in terms of the dispersion of waveguiding modes in single, isolated, nanowires, and their connection to the eigenmodes of the nanowire array. Finally, by combining semiconductors of decreasing band gap from the top to the bottom of the nanowires we found very good absorption profiles for next-generation solar cells where high energy photons are absorbed close to the top of the array and lower energy photons are absorbed closer to the bottom. This study is of importance for photovoltaics and general subwavelength optics in periodic structures.

References

[1] N. Anttu and H. Q. Xu: To be published

Luminescent plasma nanocomposites for the fabrication of photonic sensing devices

[1]F.J. Aparicio, [1]I. Blasczcyk-Lezak, [2]A. Borrás, [3]M. Holgado, [1]J.R. Sanchez-Valencia, [4]A. Griol, [5]H. Sohlström, [1]A.R. González-Elipe, [1]A. Barranco

[1]Instituto de Ciencia de Materiales de Sevilla CSIC-US, c/Américo Vespucio s/n 41092 Sevilla, Spain
[2]Swiss Federal Laboratories for Materials Testing and Research, EMPA, Thun, Switzerland
[3]Centro Láser, Universidad Politécnica de Madrid, Spain
[4] Nanophotonics Technology Center, UPLV, Valencia, Spain
[5]Royal Institute of Technology, KTH, Stockholm, Sweden
e-mail: fjaparicio@icmse.csic.es

Dye molecules embedded in different matrices in the form of thin films are the basis of specific materials used for laser cavities, optical filters, optical gas sensors, etc. Usually, the synthesis of this type of thin films is intended by sol/gel and similar wet methods and the films use to have a thickness of several microns. These procedures present some drawbacks as, for example, the need of different steps for drying, annealing, etc. Other limitations come from the microstructure of the films (e.g., surface roughness), that may impose some restrictions when these materials have to be integrated in optical and photonic devices. On the other hand the vacuum deposition of dye molecules produce films formed by small light dispersing crystalline aggregates with very poor optical and mechanical properties.

In the present communication we discuss a new methodology based on the plasma polymerization of dye molecules that circumvent the above mentioned problems [1-3]. It permits a tailored synthesis of optically active nanometric thin films containing dye molecules which are active as fluorescence emitters (i.e., coloured and fluorescent films). The principle of this new procedure is the partial polymerization of dye molecules that are evaporated over a substrate while exposed to a remote Ar plasma. As a result of this process a polymeric thin film is produced in one step where some dye molecules keep intact their optical activity (although eventually, their optical response can be slightly modified by matrix effects). This methodology has been recently used for the deposition of novel plasma nanocomposites containing non-aggregated laser dyes to maximize the fluorescent emission of the materials [1, 2] and for the fabrication of optical NO_2 sensing nanocomposites [3].

To illustrate the possibilities of the technique we present here results for different fluorescent dye molecules, as perylene dyes, and several xanthene and oxazine derivative cationic dyes which are typically used as gain media in tuneable laser dyes. The luminescent, optical and sensing properties of these dye containing nanocomposites will be presented. These active optical layers are being developed for the fabrication of photonic sensor devices and optical filters (PHODYE Project) [4]. This is due to the full compatibility of the synthetic methodology with the present integrated microelectronic and optoelectronic technology.

References

[1] A. Barranco, P. Groening. Langmuir **22**, 6719 (2006).
[2] F.J. Aparicio et al. Plasma. Process. Polym. 1 (2009) 6, 17-26.
[3] I. Blasczcyk-Lezak, F.J. Aparicio et al. J. Phys. Chem. C (2009), 113, 431–438.
[4] New photonic systems on a chip based on dyes for sensor applications scalable at wafer fabrication (PHODYE EU Project) http://phodye.icmse.csic.es

Modeling switching in STM molecular junctions

T. Brumme, F. Pump, C. Toher, R. Gutierrez, and G. Cuniberti
Institute for Materials Science, TU Dresden

A broadly observed phenomenon in experiments on molecular junctions is time dependent switching of the tunneling current [1-5]. In many cases such behavior involves different current states which are attributed to the transfer of single atoms or functional groups in a molecule between different stable configurations. We describe here the investigation of the current switching observed in a molecular junction formed by a PTCDA molecule between an STM tip and an Ag(111) surface, which is believed to be due to the carboxylic oxygen atom switching between the surface and the tip [6]. We use a generalized version of a model developed in 1997 by Gao et al. [7] to investigate the results observed in these experiments. The distribution of the switching events measured in the experiments shows a power law dependence for small positive bias voltages, whereas for negative voltages it shows a constant behavior. Compared to Gao's model, which can only describe the rapid increase of the switching events at a certain onset voltage, our extended model can be used to characterize the whole distribution relating the different behavior to the changes in the potential by the applied bias.

References

[1] Z.J. Donhauser, B.A. Mantooth, K.F. Kelly, L.A. Bumm, J.D. Monnell, J.J. Stapleton, D.W. Price Jr., A.M. Rawlett, D.L. Allara, J.M. Tour, P.S. Weiss, Science 292, 2303 (2001).
[2] G.K. Ramachandran, T.J. Hopson, A.M. Rawlett, L.A. Nagahara, A. Primak, S.M. Lindsay, Science 300, 1413 (2003).
[3] M. Lastapis, M. Martin, D. Riedel, L. Hellner, G. Comtet, G. Dujardin, Science 308, 1000 (2005).
[4] B.-Y. Choi, S.-J. Kahng, S. Kim, H. Kim, H.W. Kim, Y.J. Song, J. Ihm, Y. Kuk, Physical Review Letters 96, 156106 (2006).
[5] P. Liljeroth, J. Repp, and G. Meyer, Science 317, 1203 (2007).
[6] F. Pump, R. Temirov, O. Neucheva, S. Soubatch, S. Tautz, M. Rohlfing, G. Cuniberti, Appl. Phys. A 93, 335 (2008).
[7] S. Gao, M. Persson, and B. Lundqvist, Phys. Rev. B 55, 4825 (1997).

Amplitude- and phase-resolved optical near fields of propagating surface plasmons on extended and nanostructured thin films

T. V. A. G. de Oliveira †, J. Dorfmüller, R. Vogelgesang, K. Kern

Max-Planck-Institute for Solid State Research, D-70569 Stuttgart, Germany
† New Address: Self-Assembly Laboratory, CIC nanoGUNE Consolider, E-20018 San-Sebastián, Spain
Spaint.oliveira@nanogune.eu

In conventional implementations of apertureless Scanning Near-field Optical Microscopes, sample excitation is accomplished through the same lens used to collect backscattered near field signals [1]. The main advantage of this illumination scheme is that excitation and collection foci share the same volume, thus facilitating illumination alignment procedure. High intensity of detected fields and excellent resolution are among the qualities of this solution. Many interesting optical phenomena, however, cannot be exploited with this type of excitation. In plasmonics, for instance, this solution is limited to the investigation of SPR in small particles – also known as particle plasmons. If the structure supporting SPR is too large compared to the beam focus waist, propagation of SPP prevails in detriment of cavity resonances. Consequently, as the map of near fields is acquired always in the exact position where SPP is coupled, the interpretation of the resulting image gets complicated [2].Here I present a new illumination scheme, wherein sample illumination is completely independent of the collection lenses. Light excites the structures of interest through the glass substrate supporting them. Specifically, I have investigated the capability of a SNOM in the study of Propagating Surface Plasmons on extended and structured thin films deposited on glass substrates. Exploiting the strong analytical potential of the instrument, near-field phase and intensity maps of the local fields has allowed the direct measurement of wave vectors associated with the propagating SPP on thin films, as seen in Figure 1 [3].

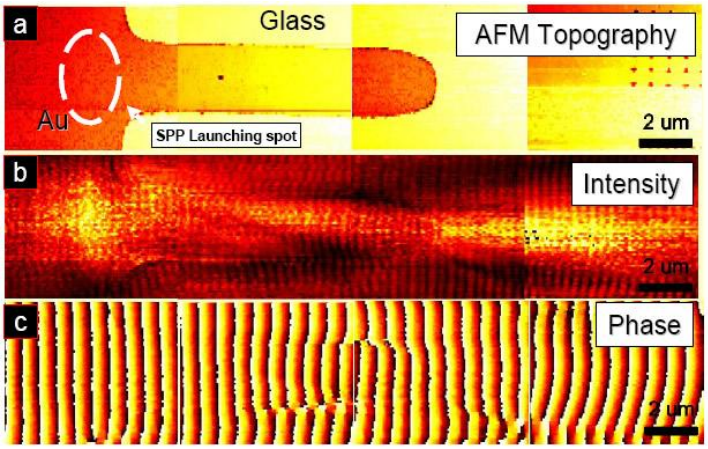

Figure 1: *SPP propagation on metal stripe. In (a) the topography image, wherein darker regions represent higher features. SPP is coupled to the metal surface on the region indicated by the white circle. Optical near-field amplitude and phase are depicted in (b) and (c), respectively. The wavelength in vacuum of the light used was = 820nm.*

References

[1] Hillenbrand, R. PhD Thesis, Technische Universität München, 2001.[2] Vogelgesang, R.; Dorfmüller, J.; Esteban, R.; Weitz, T.; Dmitriev, A.; Kern, K. Phys. Stat. Sol. (b), 245, p. 2255-2260, 2008.[3] de Oliveira, T. V. A. G. Diploma Thesis. Universidade Federal de Santa Catarina, 2008.

Interaction between LSP and SPP in magnetoplasmonic structures

J. F. Torrado[1], J. B. González-Díaz[1], A. García-Martín[1], M. U. González[1,2], J. M. García-Martín[1], A. Cebollada[1], S. Acimovic[2], J. Cesario[2], R. Quidant[2], G. Badenes[2], G. Armelles[1]

[1]Instituto de Microelectrónica de Madrid, CSIC, Tres Cantos, Madrid, Spain
[2]ICFO-The Institute of Photonic Sciences, Castelldefels, Barcelona, Spain
email: antonio@imm.cnm.csic.es

Summary

In this work we study the effect of localized plasmon excitation on the response of a magneto-optically active system that also supports extended plasmons (magneto-plasmonic thin film). It is carried out using two different configurations for the applied magnetic field, and its influence on both kinds of plasmons is also analyzed.

Introduction

It is well known that the fundamental optical properties of hybrid structures conformed by arrays of metallic nanoparticles, sustaining localized surface plasmons (LSP), and metallic films, which support propagating surface plasmons (SPP), are strongly influenced by their mutual electromagnetic coupling [1,2]. On the other hand, the inclusion of ferromagnetic materials in nanoparticles or metallic films allow us to control the respective excitation LSP and SPP by an external magnetic field [3,4]. In this work we analyze a system presenting both situations: LSP on gold nanoparticles over a continuous metallic trilayer exhibiting magneto-optical (MO) activity.

Discussion

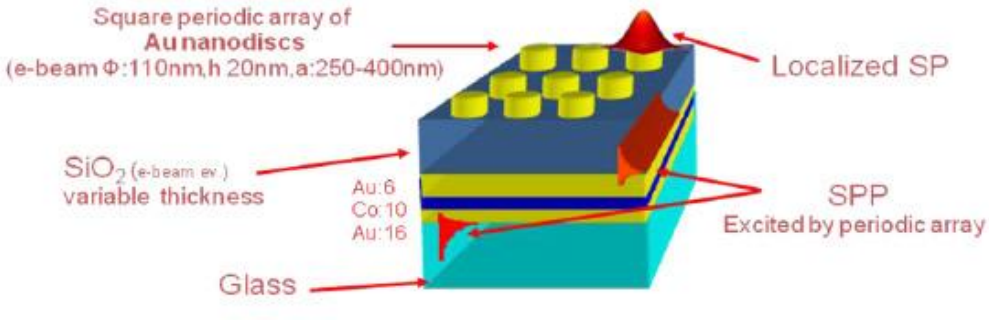

Figure 1: *Configuration sustaining LSP, SPP and magneto-optical activity analyzed in this work.*

Figure 1 shows the system under study: a Au/Co/Au trilayer film over a glass substrate and below a thin SiO_2 spacer that has an array of gold nanoparticles on top of it. The magneto-optical response of samples with different thicknesses of SiO_2 and different array periodicities have been measured in both the polar Kerr and the transverse Kerr configurations. In the polar Kerr configuration we analyze the polarization conversion (p-light into s-light) in the reflected light when a magnetic is applied perpendicular to the sample plane and parallel to the incident light plane; and in transverse Kerr measurement, we study the modification of the intensity of the reflected p-light when the magnetic field is applied parallel to the sample plane and perpendicular to the incident light plane.

The polar Kerr results show that the MO response differs from that of the trilayer alone due to the presence of LSP, even being physically separated. Moreover, we have determined that there is a redistribution of the electromagnetic field inside the trilayer when the LSP is excited, resulting in an enhancement of the MO signal only for those energies where the electromagnetic field is increased [5].
In the transverse Kerr configuration both the LSP and SPP plasmons are excited, and from the dependence on the angle of incidence of the TMOKE spectra, we can reconstruct the SPP dispersion relation. In this configuration the magnetic field introduces a modulation of the SPP wavevector allowing thus the use an external magnetic field as a tuning parameter of SPP properties. Furthermore, in the spectral region where both plasmon modes interact, this effect is reduced and partly transferred to the LSP.

Conclusions

We have studied the influence of the excitation LSP on the MO activity of the system, the effect of the magnetic field on both kind of plasmons, and the mutual interaction between them, finding an enhancement of the MO Kerr activity due to the plasmon excitation, and that the propagation of the SSP can be altered via modulation of its wavevector.

This work has been financially supported by the Spanish MICINN (NAN2004-09195-C04 and MAT2005-05524-C02-01), CM (Microseres and Nanomagnet) and EU (FP6/2003/IST/2-511616-Phoremost and NMP3-SL-2008-214107-Nanomagma).

References

[1] A. Christ, T. Zentgraf, S. G. Tikhodeev, N. A. Gippius, J. Kuhl, and H. Giessen, Phys. Rev. B 74, 155435 (2006).
[2] J. Cesario, R. Quidant, G. Badenes, and S. Enoch, Opt. Lett. 30, 3404-3406 (2005).
[3] J. B. Gonzalez-Diaz, A. Garcia-Martin, G. Armelles, J. M. Garcia-Martin, C. Clavero, A. Cebollada, R. A. Lukaszew, J. R. Skuza, D. P. Kumah, and R. Clarke, Phys. Rev. B 76, 153402 (2007).
[4] J. B. González-Díaz, A. García-Martín, J. M. GarcíaMartín, A. Cebollada, G. Armelles, B. Sepúlveda, Y. Alaverdyan, and M. Käll, Small 4, 202-205 (2008).
[5] G. Armelles, J. B. González-Díaz, A. García-Martín, J. M. García-Martín, A. Cebollada, M. U. González, S. Acimovic, J. Cesario, R. Quidant, and G. Badenes, Opt. Express 16, 16104-16112 (2008).

Atomically structured metallic nanowires on the kBr passivated INSB surface

Szymon Godlewski, Grzegorz Goryl, Maria Goryl, Jacek Kolodziej, Franciszek Krok, Marek Szymonski

Centre for Nanometer-Scale Science and Advanced Materials, NANOSAM, Faculty of Physics, Astronomy, and Applied Computer Science, Jagiellonian University, Reymonta 4, 30-059 Krakow, Poland

In recent years organic semiconducting layers deposited on various surfaces as well as single-molecule devices have attracted considerable attention because of a rapid development of new technologies for electronics. Although computing devices based on a single-molecule concept are still at a very early design stage they attract more and more attention. The demand to functionalize logically and control electronically organic molecules requires application of very complex templates. The existence of different adsorption sites would enable to connect or isolate electrically the molecules from the substrate. In our talk we will present the novel template for organic molecules deposition. The template consist of semiconducting InSb(001) c(8x2) reconstructed substrate covered with insulating KBr pseudomorphic thin layers with atomically structured metallic nanowires created during gold deposition. We will present atomically resolved LT-STM (obtained at 77K) images and discuss the properties of the whole system including the properties of the insulating thin KBr layers (thin film epitaxial growth and superimposed interface states structures) and metallic contacts (creation of In-Au alloy). The electronic properties will be discussed on the basis of STM/STS measurements.

Acknowledgments

This work was supported by the Polish Ministry of Science and Higher Education under contract no. 0398/P03/2005/29 and the European Commission within the Integrated Project, ‘Computing Inside Single Molecule Using Atomic Scale Technologies, Pico-Inside’, contract no. 015847.

III-N nanostructures for Intersubband optoelectronics

P. K. Kandaswamya[*, C]*. Bougerol*[b]*,H. Machhadani*[c]*, M. Tchernycheva*[c]*, F. H. Julien*[c]*, A. Vardi*[d]*, G. Bahir*[d]*, and E. Monroy*[a]

[a]*CEA-Grenoble, INAC/SP2M/NPSC, 17 rue des Martyrs, 38054 Grenoble, France*
[b]*Institut Néel-CNRS, NPSC, 25 rue des Martyrs, 38042 Grenoble, France.*
[c]*Institut d'Electronique Fondamentale, Université Paris-Sud, 91405 Orsay, France*

Intersubband (ISB) technology achieved a major milestone when the first InAlAs/InGaAs quantum cascade (QC) laser was demonstrated. Unlike the interband devices whose operating wavelength depends on the band gap, ISB offers possibilities of wavelength control by design, since it involves transitions between the confined states of quantum wells (QW). Owing to many advantages of the ISB technology, much effort was focussed trying to push the operation wavelength towards telecommunication spectral range. Using the GaN/AlN system, we can easily reach this technologically important wavelength thanks to the large conduction band offset of 1.75 eV. Other advantage of these semiconductors is the prospects for ultrafast ISB devices operating at multi-Tbit/s data rates due to short recovery times (~ 200fs), possible by strong Frohlich interaction in III-N. In this abstract we will discuss the various material issues, followed by a description of devices in near-IR (NIR) region. The advantage of using polar or semipolar materials for our application, and the current status of nitride-based ISB technology for the mid-IR (MIR) will also be addressed.

The growth of the structures was performed on AlN-on-sapphire templates using plasma-assisted molecular beam epitaxy with in-situ monitoring by reflection high energy electron diffraction. The large lattice mismatch of 2.4% between GaN/AlN demands critical tuning of growth conditions. Thus, to reduce relaxation through channels like threading dislocations and periodic stacking faults, we have adopted methods like supplying Ga excess during the deposition of GaN and AlN, which reduces the surface energy and increases the mobility of the adsorbed species [1]. Taking advantage of sapphire transparency in the NIR, we have demonstrated charge transfer electro-optical modulators with modulation depth of 14dB -enough to achieve 10-12 bit error rate-, polarization induced phonon ladder QC detectors [2] with a responsivity of 10 mA/W and RC limited -3dB bandwidth greater than 10 GHz, and intraband quantum dot photodetectors. Figure 2 clearly shows the energy levels placed in resonance with the phonon energy of ~ 90 meV, allowing rapid relaxation.

Although polar structures offer many advantages, like a polarization-induced enhancement of the conduction-band offset, there are some potential disadvantages - for example, the wavelength shift and the corresponding reduction in oscillatory strength when operated under bias- which can be overcome by using semipolar-oriented structures. As a step in this direction we recently reported the first observation of ISB absorption from semipolar GaN/AlN SLs.

The III-N ISB technology not only finds application in the NIR wavelengths, as described above, but it also offers the flexibility to fabricate devices in the MIR range and even further, upto possibly the Terahertz range. Using an 8 band k.p Schrödinger poisson solver we have theoretically predicted the suitable structural parameters required for ISB transition at MIR region. The red shift of transition energy can be achieved on reduction of electric field and quantum confinement in the well, by decreasing the Al content in the barrier and increasing the well width. We have performed the growth of the structures absorbing at MIR on semi-insulating Si(111), to avoid the absorption by the substrate. Experimental measurements of the ISB transition energy show good agreement with our calculatins. The observed

experimental ISB absorption can be tuned up to 10 μm, with the spectral width falling between 15-20% -comparable to Arsenic system with values between 10-15% [4].

References

[1] P. K. Kandaswamy, et al., J. Appl. Phys. 106, 013526 (2009)
[2] A. Vardi, et al., Appl. Phys. Lett. 93, 193509 (2008).
[3] Nextnano3 http://www.nextnano.de/nextnano3/
[4] P. K. Kandaswamy, et al., J. Appl. Phys. 106, 013526 (2009)

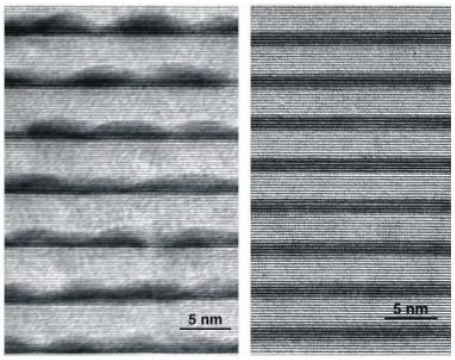

Figure 1: *High-resolution TEM images of (0001)-oriented GaN/AlN QD (left) and QW (right) superlattices.*

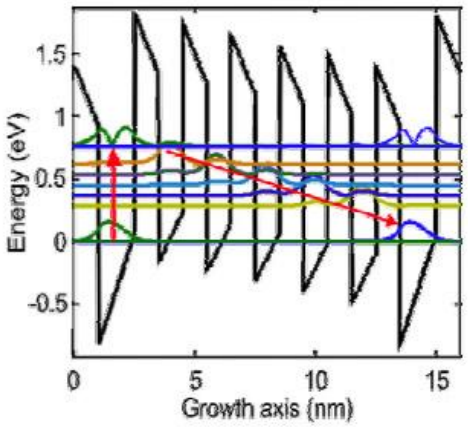

Figure 2: *Band diagram and energy levels in one stage of the structure. (Red arrow) direction of electron relaxation (Bold lines) denote states involved in optical transitions.*

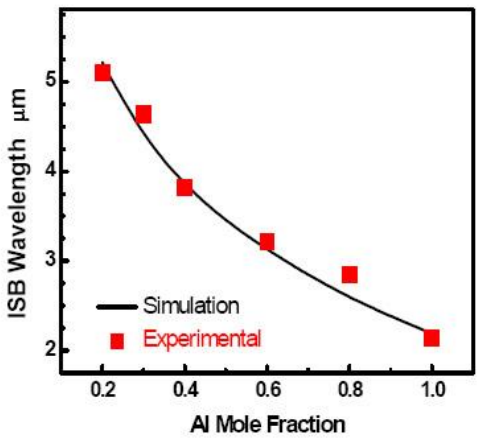

Figure 3: *Variation of ISB transition energy with Al mole fraction on the barrier*

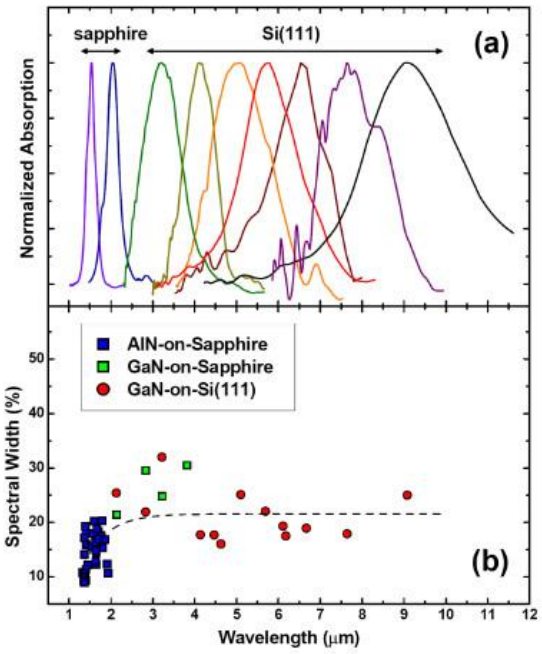

Figure 4: *(a). IR absorption spectra for TM-polarized light measured in GaN/Al(Ga)N superlattices grown either on sapphire or on Si(111) templates. (b) spectral width of the samples absorbing from NIR to MIR range.*

Acousto-plasmonic hot spots in metallic nano-objects

Nicolas Large[1, 4,] Adnen Mlayah[1], Lucien Saviot[2], Jérémie Margueritat[3], José Gonzalo[3],Carmen N. Afonso[3], and Javier Aizpurura[4]

[1]Centre d'Elaboration des Matériaux et d'Etudes Structurales CEMES – CNRS, Toulouse, France
[2]Institut Carnot de Bourgogne, UMR 5209 CNRS-Université de Bourgogne, Dijon, France
[3]Laser Processing Group, Instituto de Optica, CSIC, Madrid, Spain
[4]Donostia International Physics Center DIPC & Centro Mixto de Física de Materiales CSIC-UPV/EHU, San Sebastian, Spain

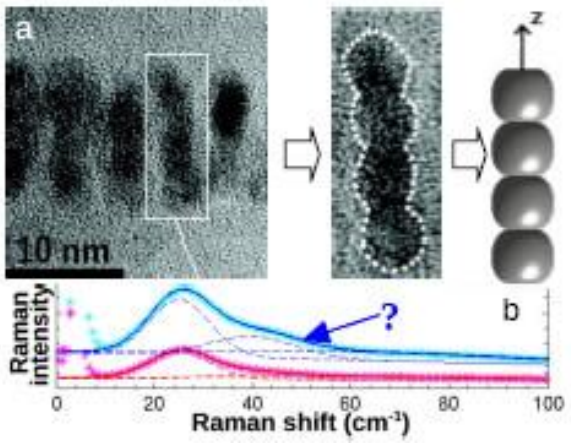

Figure 1: *(a) TEM images of silver NCls and the modelled indented NCl. (b) Raman spectra of the NCls.*

In this work we investigate the acousto-plasmonic dynamics of metallic nano-objects by means of resonant Raman scattering. Acousto-plasmonic interactions still presents several theoretical challenges to correctly interpret the Raman-Brillouin scattering. A variety of theoretical and experimental works have been devoted to the study of shape, size, matrix and ordering effects on the surface plasmons whereas there are only few studies of the dynamical properties of the surface plasmons such as coupling mechanisms to the acoustic vibrations [1], renormalization and damping effects or inelastic light scattering properties.

The issue

We experimentally observe an unexpectedly strong acoustic vibration band in the Raman scattering (Figure 1b) of silver nanocolumns (NCls) (Fig. 1a), usually not found in isolated nano-objects. The frequency and the polarization of this unexpected Raman band allow us to assign it to breathing-like acoustic vibration modes. To understand this “anomalous” Raman scattering (“?” on Figure 1b), we address a theoretical and experimental study of the interactions between acoustic vibrations (Figure 2a) and surface plasmons (Figure 2b) [2-4]. The modulation of the surface plasmon nearfield (Figure 2c) allows for the interpretation of experimental Raman-Brillouin spectra in these objects.

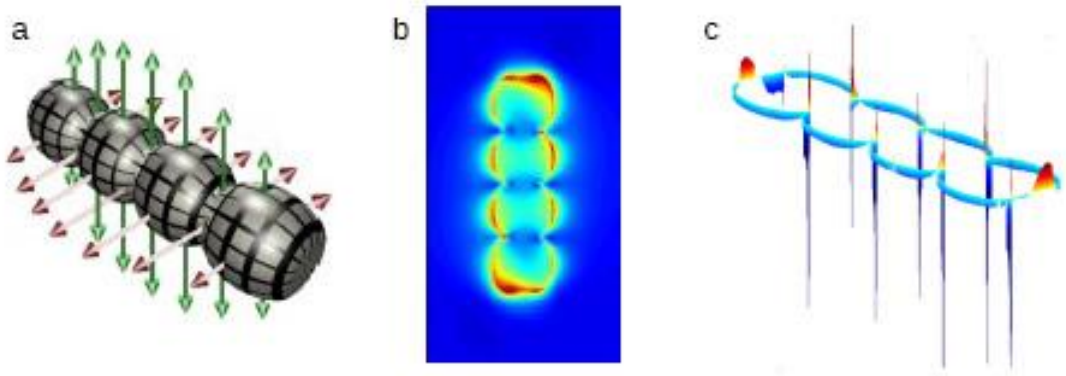

Figure 2: *(a) Displacement field of the breathing-like acoustic vibrations. (b) Surface plasmon nearfield for silver indented NCls. (c) Relative modulation of the surface plasmon polarization by the breathing-like acoustic vibrations δvibP(r)/P0(r).*

Methods

Based on full electromagnetic near-field calculations coupled to the elasticity theory, we introduce a new concept of “acousto-plasmonic hot spots” which arise here because of the indented shape of the nanocolumns. These hot spots combine both highly localized surface plasmons and strong shape deformation by the acoustic vibrations at specific sites of the nano-objects. In order to investigate this new concept, we integrate the Boundary Element Method [5,6] for the electromagnetic calculations (Figure 2b) and the elasticity theory by the means of the RUS method [7] for the vibrational calculations (Figure 2a), which allows calculating the modulation of the surface plasmon polarization for these acoustic vibrations (Figure 2c)

Results & Conclusions

We show that the interaction between breathing-like acoustic vibrations and surface plasmons at the “acousto-plasmonic hot spots” is strongly enhanced, turning almost silent vibration modes into efficient Raman scatterers. The indentations of the silver NCls are responsible for the strong localization of the surface plasmon nearfield and its modulation by breathing-like acoustic vibrations. The concepts, the numerical and experimental approaches developed in this work are not specific to indented NCls. They can be extended to other isolated nano-objects exhibiting strong field localization, to dimers of nano-objects and to more complex metallic nanostructures combining size, shape and interaction effects.

References

[1] G. Bachelier and A. Mlayah, Phys. Rev. B 69, 205408 (2004)
[2] G. Bachelier, J. Margueritat, A. Mlayah, J. Gonzalo, and C. N. Afonso, Phys. Rev. B 76, 235419 (2007)
[3] J. Margueritat, J. Gonzalo, C. N. Afonso, A. Mlayah, D. B. Murray and L. Saviot, Nano Lett. 6, 2037 (2006)
[4] J. Burgin et al, Nano Lett. 8, 1296 (2008)
[5] F. J. Garcia de Abajo et al, Phys. Rev. Lett. 80, 5180 (1998); Phys. Rev. B 65, 115418 (2002).
[6] J. Aizpurua et al. Phys. Rev. Lett. 90, 057401 (2003).
[7] W. M. Visscher et al, J. Acoust. Soc. Am. 90, 2154 (1991)

Electronic and transport properties of graphene due to its functionalization using dopants, chemical groups or metallic clusters

Nicolas Leconte
Université Catholique de Louvain (UCL) / Unité de Physico-Chimie et de Physique des Matériaux (PCPM)
Borsbeek, Belgium

Graphene exhibits extraordinary structural and electronic properties and is thus a promising candidate for various fields in nanotechnology such as nanoelectronic devices, gas sensing or even as a catalytic substrate (when its atomic structure is modified). The goal of the present work consists in investigating using first-principles techniques how the properties of graphene can be tuned using chemical functionalization or when its surface is decorated with metallic nanoclusters.

At first, the quantum transport properties of graphene nanoribbons have been calculated in presence of hydroxide (OH-) and hydrogen (H+). The quantum conductance is found to be altered by these chemical groups which play the role of scattering centers. Indeed, some specific conduction drops can be observed either at the right or at the left of the Fermi energy, depending on the nature of the impurities. Consequently, our calculations suggest the possible use of these graphene-based devices as pH nanosensors.

Secondly, the interaction of small gold clusters with defected graphene (including vacancies) has been studied ab initio in order to check the modification of their catalytic properties. Small gold clusters are known to preferentially adopt a planar structure in free space, but their atomic structure is not reported in presence of a planar substrate. The role of the vacancy defect consists in pinning the gold cluster at the graphene surface. Our ab initio calculations predict that these small clusters conserve their stable planar configuration on top of the graphene sheet. The only gold atom actively participating in the bonding is located above the carbon vacancy, thus linking the gold cluster to the hexagonal carbon network. An important electronic charge is found to be localized on that gold atom and the three connected first-nearest neighboring carbon atoms. This important charge transfer observed in gold nanoclusters on graphene could induce an enhancement of their catalytic activity when compared to conventional freestanding clusters.

Study the phonon transport by using the real space KUBO method

Wu Li
TU Dresden, Chair of materials science and nanotechnology
Dresden, Germany

We proposed employing the real space Kubo method, which has already been well applied to the electron transport, to study the phonon transport. As an application of this method, we calculated the phonon mean free path in carbon nanotube system. The result is shown to be in good agreement with the one obtained by the GF formulism, with the exception of low frequency, which is due to the limitation of computation time.

Quantum master equation for the study of electronic transport in organic systems.

Pedro David Manrique Charry
TU Dresden/ Material sciences
Dresden, Germany

We calculate a non Markovian master equation for electronic transport through organic systems including the interaction of external bosonic degrees of freedom. Within this formalism we calculate the expression for the time dependent current (TDC) as the variation of the particle number of the electrodes (fermionic baths) at arbitrary temperatures. Some partial results for the TDC are shown for different values of boson coupling, in which we found significant changes at very short time evolution. In addition, for organic systems we calculate the total energy for different geometric configuration using density functional tight binding (DFTB) including the dispersion energy correction and contrasted the results with MP2 methods finding a very good agreement.

Two-dimensional surface emitting photonic crystal laser with hybrid triangular-graphite structure

L. J. Martínez[a], B. Alén[a], I. Prieto[a], C. Seassal[b], P. Viktorovitch[b], L. E. Muñoz [a], J.F. Galisteo-López[c], M. Galli[c], L.C. Andreani[c] and P.A. Postigo[a]

[a]Instituto de Microelectrónica de Madrid (IMM-CNM- CSIC), Isaac Newton 8, E-28760, Tres Cantos Madrid, Spain
[b]Institut des Nanotechnologies de Lyon (INL) UMR 5270 CNRS-ECL-INSA-UCBL Ecole Centrale de Lyon 36, Avenue Guy de Collongue F - 69134 Ecully Cedex
[c]Dipartimento di Fisica "A. Volta" and UdR CNISM, Universit`a degli Studi di Pavia, via Bassi 6, I-27100 Pavia, Italy
Contact e-mail: ivanpg@imm.cnm.csic.es

Laser emission of a compact surface-emitting microlaser, optically pumped and operating around 1.55 μm at room temperature is presented. The two-dimensional photonic crystal is conformed in a hybrid triangular-graphite lattice designed for vertical emission. The structures have been fabricated on InP slabs. The heterostructure consists of four *In0.65As0.35P/InP* quantum wells grown on an InP substrate by molecular beam epitaxy and it is transferred onto a silicon-on-silica substrate by wafer bonding (SiO_2 thickness = 0.9±0.1mm). Standard techniques of electron-beam lithography, reactive ion beam etching and reactive ion-etching have been used for the patterning. The optical characterization was performed by micro-photoluminescence spectroscopy. Single-mode, strongly polarized laser emission has been achieved with quality factors Q exceeding 12000. In this work we show laser emission from the hybrid triangular-graphite lattice at the Γ point. This lattice was introduced with the aim of combined the good properties of the triangular and graphite lattice [1]. The structure has several bands with slow curvature close to the high symmetry points. The lattice was fabricated in III-V semiconductor slab [2]. The structure presents a strong photoluminescence around 1500 nm. The hybrid triangular-graphite lattice was fabricated with lattice parameters R/a=0.12, Rg/a=0.17, and several values of a=840-1050nm at steps of 20nm. Guide-mode expansion method for band calculation [3] has been used. The structures are fabricated on squares with sides around 30 μm. Polarization resolved micro-photoluminescence spectroscopy was used for optical characterization. The samples were optically pumped with a 780nm laser diode through a NA=0.14 (5x) objective placed at normal incidence. The PL emission was collected by a fiber coupled to a optical spectrum analyzer. Several lasing devices operating around 1.55μm with thresholds of a few of hundreds of microwatts showing polarized emission have been measured.

References

[1] L.J. Martínez, A. García-Martín, and P. A. Postigo, Opt. Express 12 (23), 5684-5689 (2004).
[2] C. Monat, C. Seassal, X. Letartre, P. Regreny, M. Gendry, P. Rojo Romeo, P. Viktorovitch, M. Le Vassor d'Yerville, D. Cassagne, J. P. Albert, E. Jalaguier, S. Pocas, and B. Aspar, J. Appl. Phys. 93, 23 (2003).
[3] L. C. Andreani and D. Gerace, *Phys. Rev. B*, 73, 235114, 2006.

Study of SB-MOSFETs on SOI substrates

J.L. Padilla[1] and F. Gámiz[1]
[1]Departamento de Electrónica y Tecnología de los Computadores
Universidad de Granada, Facultad de Ciencias. Avda Fuentenueva s/n, Spain
Email: jluispt@ugr.es , fgamiz@ugr.es

This work constitutes a first approach to the study of SB-MOSFETs on SOI performing several simulations that take into account the different carrier transport mechanisms that may be found in these sort of devices. Some comparisons are made depending on the mechanism considered as well as for several Schottky barrier heights and different drain and gate bias.

In SB-MOSFETs we replace conventional doped semiconductor regions by metallic materials that create rectifying metal-semiconductor junctions (Schottky barriers). These junctions having very similar electrical characteristics to doped pn junctions, present two most important scaling benefits: (i) Low source/drain resistivity (in usual MOSFETs as junctions depths are scaled to below 50nm, source and drain series resistances become increasingly significant), (ii) Abruptness of metal-semiconductor junctions allow very short physical channel lengths to be defined.
Schottky barriers are essentially unipolar current devices in which the carrier transport may be seen as formed by three different components: thermionic emission of carriers over the barrier, thermionic field emission of high energy carriers through the upper part of the barrier and field emission of carriers through the barrier at the Fermi level. Thus depending on the bias conditions at the junctions, one or more of these contributions will dominate carrier transport.

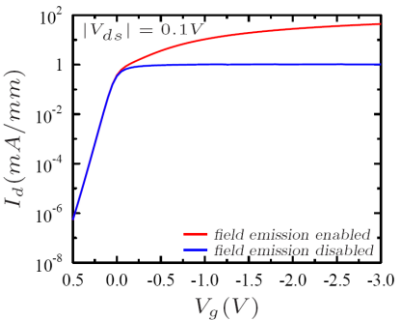

Figure 1: *Field emission enabled vs. field emission disabled for different gate bias with low drain bias.*

A first approximation to barrier height is given by [1] where $\longrightarrow$ $\begin{cases}\varphi_{bn} = \varphi_m - \chi_s \\ \varphi_{bp} = \frac{1}{q}E_g - (\varphi_m - \chi_s)\end{cases}$
In our case, we will deal with a p-channel SB-MOSFET as shown in Figure 2 therefore only holes transport will be considered. At high gate voltages, tunneling becomes determinant for current flow and consequently the higher the voltage, the narrower the barrier and field emission and thermionic field emission contributions appear. In Figure 1 it can be seen how for a gate bias of order of -3V the drain current can be nearly two orders of magnitude higher when we allow field emission mechanisms

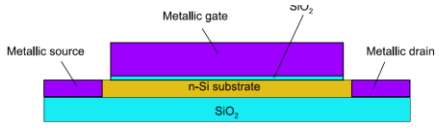

Figure 2: *p-channel SB-MOSFET with 10nm thick Si substrate. The channel length is 85nm.*

We performed oursimulations using Silvaco ATLAS software [2]. Due to the abrupt variation in electrostatic potential between metal and semiconductor in Schottky contacts, the choice of an appropriate grid is essential and thus the mesh for the simulation must be carefully designed. We choose a quite fine grid at the source-to-channel and drain-to-channel interfaces to accurately calculate the current contribution caused by field emission at the expense of greater simulation time.
The voltages applied alter the shape and height of the barriers. Increasing gate bias gives rise to higher electric fields and height of barriers is reduced due to image force lowering and dipole lowering. These two effects can be estimated using the expressions described in [3]

$$\Delta\phi_{b,ift} = \sqrt{\frac{qE_{applied}}{4\pi\varepsilon_s}}$$
$$\Delta\phi_{b,dl} = \alpha E_m$$

However, the Silvaco ATLAS simulator does not account for barrier lowering mechanisms applied to field emission but only to thermionic emission. Therefore the barrier heights used in our simulations must be regarded as zero-bias values. This approximation has negligible impact for low gate and drain biases but obviously will not accurately represent the physical processes at work for high voltages. Nevertheless, as a first approach to the behaviour of these devices, we could use these simulations and compare them to experimental data for low drain and gate bias in order to guess the most likely zero-bias barrier height.

Drain current results for a low drain bias and different zero-bias barrier heights can be seen in Figure 3. Large differences up to nearly a decade in drain current are evident at V_{gs}=-3V between the cases of 0.10 and 0.35 eV. This emphasizes the significant impact that barrier height variations have on the ON state of a SB-MOSFET.

Conversely, we can infer very small impact of barrier height on the subthreshold current. Therefore, if one considered these different zero-bias barrier heights (from 0.35 eV to 0.10 eV) as the result of a gradual barrier lowering process these results would be in agreement with the fact that barrier lowering has little effect for low gate and drain bias. The corresponding high drain voltage transfer characteristics are shown in Fig.4 in linear and logarithmic scales. In this case, as we are considering high drain bias, appreciable differences can be observed even on the subthreshold current. This again indicates that if the different barrier heights of the simulations were the effect of any barrier lowering mechanism, this mechanism becomes prominent under high drain and gate bias as expected.

We have made a first study of the behaviour of p-channel SB-MOSFETs under low and high drain/gate bias without barrier lowering effects applied to field emission calculations. Nevertheless, a convenient interpretation of the obtained results regarding the different zero-bias barrier heights introduced by hand as the result of some barrier lowering mechanism leads us to confirm the expected dramatic influence that these lowering effects have in the current of these devices. Next step will be to develop some kind of procedure as done in [4] that allows the inclusion of these effects as well as include implementation of quantum effects.

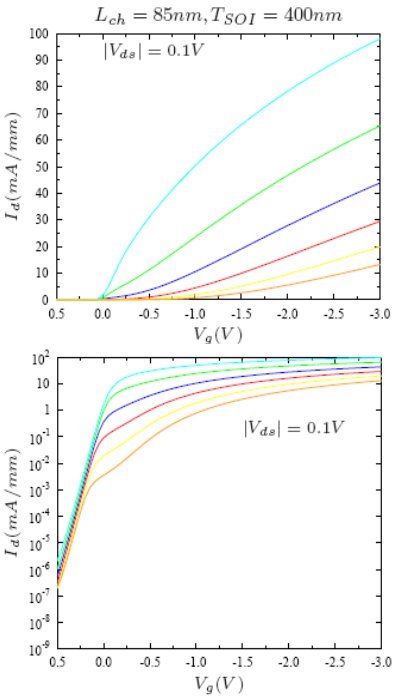

Figure 3: *Simulated drain currents for V_{ds}=0.1V for Schottky barrier heights from 0.10 eV (cyan line) to 0.35 eV (orange line). Conver*

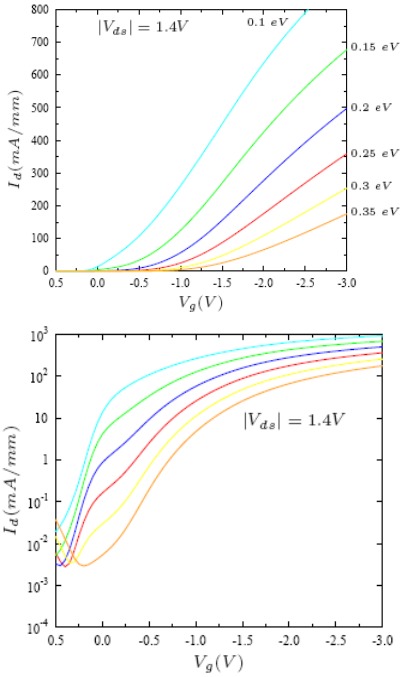

Figure 4: *Simulated drain currents for V_{ds}=1.4V for Schottky barrier heights from 0.10 eV to 0.35 eV.*

References

[1] E. H. Rhoderick and R. H. Williams. Metal-Semiconductor Contacts. Oxford Science Publications, 1988

[2] ATLAS users manual, Silvaco, 2007

[3] S. M. Sze Physics of Semiconductor Devices. Wiley, 1981.

[4] Dominic Pearman. Electrical Characterization and Modelling of Schottky barrier metal source/drain MOSFETs. Phd Thesis.

Spectroscopy of thin molecular films under ultrahigh vacuum conditions using an optical nanofiber

David Papencordt
University of Mainz, Germany

The guided modes of optical nanofibers with diameters smaller than the wavelength of the guided light exhibit a pronounced evanescent field. The absorption of light by molecules deposited at the fiber surface is therefore readily detected by measuring the fiber transmission. We have shown that the resulting absorption for a given surface coverage can be orders of magnitude higher than that for conventional surface spectroscopy. The measurements were performed on sub-monolayers of 3,4,9,10-perylene-tetracarboxylic dianhydride (PTCDA) molecules at ambient conditions, revealing the agglomeration dynamics on a second to minutes timescale [1].

We set up a new experimental apparatus which integrates the nanofiber under ultrahigh vacuum (UHV) conditions in order to gain better control over the system. Firstly, this arrangement enables us to produce a homogeneous flux of the molecules deposited onto the nanofiber. Furthermore, it allows us to desorb pollutants (water, etc.) from the fiber and thus to work with a better defined surface. The measured absorption spectra of the deposited molecules and their time evolution are compared with the results obtained at ambient conditions. Moreover, the new setup will allow us to carry out spectroscopy on a much larger variety of molecules including those not stable when sublimated at ambient conditions.

We gratefully acknowledge financial support by the Volkswagen Foundation (Lichtenberg Professorship), the ESF (European Young Investigator Award), and the EC (STREP “CHIMONO”).

References

[1] F. Warken et al., Opt. Express **15**, 11952-11958 (2007)

Formation energy of charge states of nitrogen and oxygen vacancies in anatase TiO_2: An ab initio study

M.A. Pérez-Osorio, J.M. Pruneda and P. Ordejón
CentreD'Investigació en Nanociencia i Nanotecnologia(CIN2:CSIC-ICN)
ETSE, Campus UAB,08193 Bellaterra, Barcelona, Spain.

Electronic and structural properties of several charge states of interstitial (Ni) and substitutional (Ns) nitrogen and oxygen vacancies (V_O) into anatase TiO_2 were studied through density functional theory calculations.
The formation energies indicate that different charged states happen in the range of allow edelectronic chemical potential, *μe*. ForN-doping, neutral and positively charged states occur at μe near the valence band top, namely N^0_s, N^+_s and N^{2+}_i, while negatively charged states occur at μe near the conduction band bottom, N^-_s and N^-_i.
N_i is energetically more stable than N_s and always has a negative formation energy. The presence of oxygen vacancies would facilite the formation of N^-_s because the defects levels associated to V_O can pin the Fermi level close to the bottom of the conduction band. The neutral and charged states of V_O always show positive formation energies. Vacancies with charge state 2+ have the highest stability, as has been reported in the literature.

Optical spectroscopy of conductive molecular junctions in plasmonic cavities

O. Pérez-González[1,2], *N. Zabala*[1,3], *A. Borisov*[4], *P. Nordlander*[5], *N.J. Halas*[5] *and J. Aizpurua*[2,3]

[1]*Dpt. Electricidad y Electrónica, Univ. of the Basque Country (UPV/EHU), Bilbao, Spain*

[2]*Donostia International Physics Center (DIPC), Donostia, Spain*

[3]*Centro Mixto de Física de Materiales (CSIC-UPV/EHU), Donostia, Spain*

[4] *Lab. des Collisions Atomiques et Moleculaires, CNRS-Université Paris-Sud, France*

[5]*Laboratory for Nanophotonics, Rice University, Houston, USA*

In the last decade fundamental advances have been achieved in the fields of molecular electronics [1] and plasmonics [2]. In particular, the optical properties of adjacent nanoshell pairs have been explained using exact numerical calculations and hybridization models [3]. Recent simultaneous measurements of electronic conduction and Raman spectroscopy in molecular junctions have suggested the possibility of sensing individual molecules [4], connecting both fields.

We study theoretically this connection between molecular electronics and plasmonics in a model system composed of a conductive molecular junction bridging two nanoshells. The nanoshells are formed by a silica core surrounded by a gold shell and the molecular junction is modelled as a cylinder of radius a linking both nanoshells. The conductivity of the junction, σ, is related to conductance, G, through the geometrical parameters of the system. So, for a given size of the linker, we modify the conductivity of the junction varying the number *n* of quanta of conductance, nG_0 ($G_0 \equiv 2e^2/h \cong 77.5$mS). Maxwell's equations are solved via a boundary element method (BEM) [5] to obtain the electromagnetic fields and the optical extinction spectra.

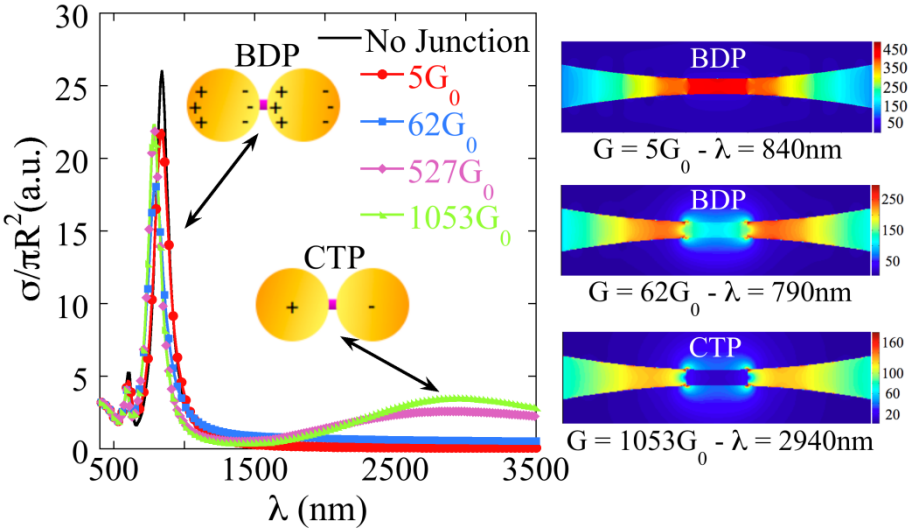

Figure 1: *(Left) - Optical extinction spectra of a nanoshell dimer bridged by a conductive molecular junction of radius a = 2nm, as conductivity is increased via the increment of conductance. We can observe the variations in the behaviour of the plasmon resonance (BDP) and the appearance of the new resonance (CTP) in the IR part of the spectrum. (Rigth) - Near-fields patterns corresponding to the short wavelength regime (up and medium) and to the long wavelength regime (down), where the progressive expelling of the electric field out of the junction can be observed.*

We find two regimes in the optical response (see Figure 1). For the short wavelength regime, we first notice a broadening of the plasmon resonance as conductance is increased until a saturation point is reached. Then, a slight blue-shift takes place and

the plasmon resonance becomes narrower again. We call this resonance the Bonding Dimer Plasmon (BDP). For the long wavelength regime, when conductance takes small values, there is no appreciable change. However, for very large values of conductance, a new highly red-shifted resonance appears. We call this resonance Charge Transfer Plasmon (CTP) and its main feature is its tunability.

We believe that the study of spectral changes in plasmonic cavities might serve as a probe of molecular conductance and transport in the visible, a regime not accessible through electrical measurements.

References

[1] T. Dadosh Y. Gordin, R. Krahne, I. Khivrich, D. Mahalu, V. Frydman, J. Sperling, A. Yacoby, and I. Bar-Joseph*, Nature* **436**, 677, (2005).
[2] J. Aizpurua, G.W. Bryant, L.J. Ritcher and F.J. García de Abajo, *Phys. Rev. B* **71**, 235420 (2005).
[3] J.B. Lassiter, J. Aizpurua, L.I. Hernández, D.W. Brandl, I. Romero, S. Lal, J.H. Hafner, P. Nordlander and N.J. Halas, *Nano Lett.* **8**, 1212 (2008).
[4] D.R. Ward, N.J. Halas, J.W. Ciszek, J.M. Tour, Y. Wu, P. Nordlander and D. Natelson, *Nano Lett.* **8**, 919, (2008).
[5] F.J. García de Abajo and A. Howie, Ph*ys. Rev. Lett.* **80**, 5180 (1998).

Light processing of nanoporous semiconducting oxides for the fabrication of optically active thin films

J.R. Sánchez-Valencia[1], A. Borrás[1,2], V.J. Rico[1], S. Hamad[1] , A. Barranco[1], J.P. Espinós[1], A.R. González-Elipe[1]

[1] Instituto de Ciencia de Materiales de Sevilla (CSIC-Univ. Sevilla), Spain
[2] Nanotech@surfaces Laboratory, EMPA Materials Science and Technology, Thun, Switzerland.
Corresponding author e-mail: jrsanchez@icmse.csic.es

UV illumination of semiconducting oxides as TiO_2 and Ta_2O_5 has been proved as an effective procedure for enhancing the photo-activity of these materials in a subsequent photo-activated process [1-2]. However, despite the existing literature, to our knowledge there have been no systematic studies trying to explore the possibilities of using the illumination of these materials surfaces as an additional tool for developing new processing procedures. In this communication we present a series of experiments showing how the irradiation of these thin films behave differently face to the preparation of composite materials prepared by infiltration. This investigation has been carried out with porous TiO_2 and Ta_2O_5 thin films prepared by Plasma Enhanced Chemical Vapour Deposition (PECVD) and/or Electron Evaporation procedures [2]. These layers present well controlled porosities consisting of meso- and/or micropores. The preparation of two types of functional nanocomposite materials is intended by infiltration. They consist of dye (Rhodamine 6G and Rhodamine 800) molecules used as laser dyes and silver in the form of nanoparticles, both of them embedded within the semiconducting thin films. Dye thin films in mesoporous semiconducting thin films have been proposed for good candidate for laser materials [3]. Silver particles presenting well resolved plasmon structures have been also studied because of their interesting applications as sensor and “camaleonic” materials [4]. In the present work, we studied the relation between thin film microstructure, optical properties, surface energy variations and the distribution of the dye/metal nanoparticules when the layers are exposed to post-deposition light irradiation treatments. We believe that the reported findings open new ways for a tailored synthesis of composite optical materials.

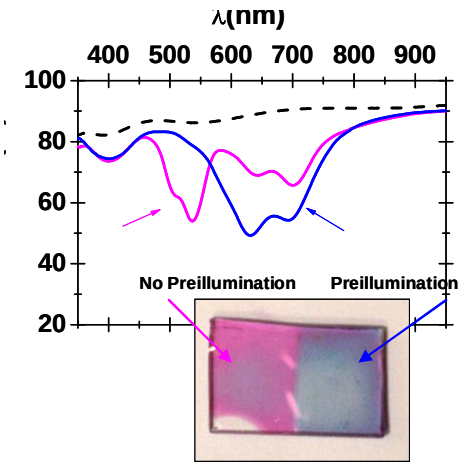

Figure 1: *UV-vis transmission spectra of Ta_2O_5 thin films immersed in a solution of Rh 6G and Rh-800 for pre-illuminated and non illuminated samples.*

References

[1] V. Rico, C. López, A. Borrás, J.P. Espinós, A. R. González-Elipe. Solar Energy Mater. Solar Cells, 90 (2006) 2944
[2] A. Borrás, A. Barranco, A.R. González-Elipe. J. Mater. Sci. 41 (2006) 5220
[3] R. Vogel, P. Meredith, et al. ChemPhysChem. 4 (2003) 595
[4] J. Homola, S.Y. Sinclair, G. Gauglitz. Sensors and Actuators B 54 (1999) 3.

Control of local near fields in optical antennas by load engineering: bridging the gap

Martin Schnell[1], Aitzol García-Etxarri[2], Andreas Huber [1,3], Ken Crozier[4], Javier Aizpurua[2], Rainer Hillenbrand [1,3]

[1] Nanooptics Laboratory, CIC nanoGUNE, 20009 Donostia - San Sebastian, Spain
[2] Donostia International Physics Center (DIPC) and Centro Mixto de Fisica de Materiales (CSIC-UPV/EHU), 20018 Donostia – San Sebastian, Spain
[3] Max-Planck-Institut für Biochemie, 82152 Martinsried, Germany
[4] Harvard University, School of Engineering and Applied Sciences, Cambridge MA 02138, USA
m.schnell@nanogune.eu

Transmission-mode scattering-type near-field optical microscopy (s-SNOM) is applied for mapping the near-field distribution in amplitude and phase of infrared nanoantennas that are loaded with metallic bridges at their central gap. By varying the size of the bridge we trace the changes in the near-field distribution of the antennas, showing that targeted antenna loading is a promising means to engineer local near fields.

Our s-SNOM [1] is based on an atomic force microscope (AFM) where a dielectric Si tip scatters the local near fields of the antenna structures. Homogeneous antenna illumination from below through the substrate (transmission mode) avoids phase-retardation effects inherent to the backscattering geometry in typical s-SNOM experiments. In combination with a pseudoheterodyne interferometric detection scheme [2], we are able to map the near-field distribution in both amplitude and phase.

The experiments were performed with gold nanorods (1550nm x 230nm x 60nm) designed for fundamental dipolar resonance at λ = 9.6 µm [3]. By focused-ion-beam (FIB) milling at the center of the nanorods, we fabricated narrow, electrically isolating gaps. Loading the gap with metallic bridges was achieved by only partially FIB milling, leaving a small gold bridge of variable size at the gap that still electrically connects both antenna segments. With s-SNOM imaging the rods at the fixed wavelength of λ = 9.6 µm, we monitor the changes in the amplitude and phase of the near-field patterns.

The near-field images of the unmodified nanorod (Figure 1a) show the fundamental dipolar near-field mode of a λ/2 antenna [4], yielding high amplitudes at the antenna extremities and a phase jump of 180° at the center of the antenna. By introducing an 80 nm wide isolating gap (Figure 1c), the near-field mode splits up into two dipolar-like modes. A highly interesting near-field distribution is observed with the nanorod loaded with a tiny metal bridge (Figure 1b). The amplitude signal on the antenna surface is always non-zero, including at the gap. Apparently, the gap is not short-circuited despite of the electrical connection made by the metal bridge. Moreover, a prominent phase gradient of 80° is observed along the antenna

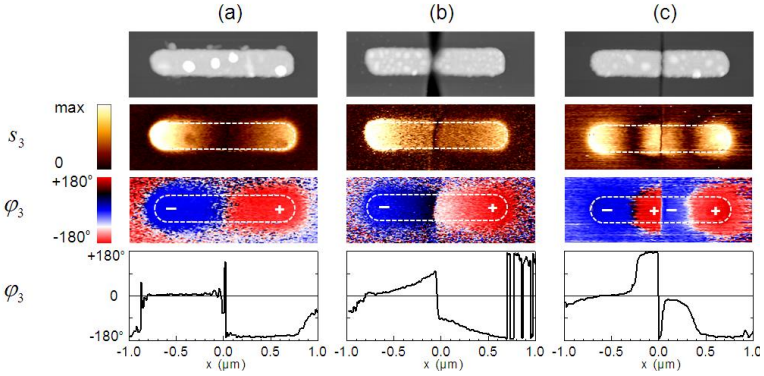

Figure 1: *(from top to bottom) Topography, IR near-field amplitude s_3 and phase φ_3 images, line plot of phase φ_3 along the antenna axis.*

segments (see line plot), indicating a time delay between the near fields at the gap and the antenna extremities. Obviously, the near-field distribution depends very much on the characteristics of the gap load. Antenna loading provides an excellent means to locally control near fields which can have successful application in the development of compact and integrated nano-photonic devices.

References

[1] F. Keilmann, and R. Hillenbrand, Philosophical Transactions of the Royal Society A 362, 787 (2004).
[2] N. Ocelic, A. Huber, and R. Hillenbrand, Applied Physics Letters 89, 101124 (2006).
[3] K. B. Crozier et al., Journal of Applied Physics 94, 4632 (2003).
[4] J. Aizpurua et al., Physical Review B 71, 235420 (2005).

Ultra-sensitive fluorescence spectroscopy of isolated surface-adsorbed molecules using an optical nanofiber

Ariane Stiebeiner
University of Mainz, Germany

The strong radial confinement and the pronounced evanescent field of the guided light in optical nanofibers allow the controlled interaction with particles which are deposited near or on the fiber surface. We have demonstrated that surface absorption spectroscopy of molecules using nanofibers is several orders of magnitude more sensitive than conventional methods based on free beam absorption [1].

Using the guided mode of the nanofiber for excitation and fluorescence collection, we present spectroscopic measurements on 3,4,9,10-perylene-tetracarboxylic dianhydride molecules (PTCDA) at ambient conditions. The fluorescence light emitted by the molecules adsorbed on the fiber surface is efficiently coupled into the guided mode of the fiber yielding a high degree of sensitivity for spectroscopic studies. Surface coverages as small as 0.1 % of a compact monolayer still give rise to fluorescence spectra with a good signal to noise ratio. We perform interlaced measurements of absorption and fluorescence spectra in order to determine the respective surface coverage.
The characteristics of our system result in self-absorption, i.e., a partial reabsorption of the emitted fluorescence by circumjacent molecules along the nanofiber. While the high sensitivity of our method allows us to perform measurements in a regime of low surface coverages where self-absorption is negligible, it is taken into account for higher surface coverages.

Moreover, upon excitation at the low energy edge of the absorption spectrum, we observe fluorescence emission at wavelengths smaller than the excitation wavelength. We attribute the occurrence of this so-called anti-Stokes fluorescence to the thermalization of the internal degrees of freedom of the molecules with the fiber surface. In order to investigate the temperature dependence of this effect, we are currently setting up an apparatus for measurements in a cryogenic environment. The new setup together with the high sensitivity of our method would allow us to perform nanofiber-based spectroscopy on the single molecule level.

We gratefully acknowledge financial support by the Volkswagen Foundation (Lichtenberg Professorship), the ESF (European Young Investigator Award), and the EC (STREP “CHIMONO”).

References

[1] F. Warken et al., Opt. Express **15**, 11952-11958 (2007)

Nanoscale infrared near-field mapping of free-carrier concentration in single semiconductor nanowires

J.M. Stiegler[1], A.J. Huber[1,2], S.L. Diedenhofen, J. Gomez Rivas[3], R.E. Algra[4,5], E.P.A.M. Bakkers[6], R.Hillenbrand[1,2]

[1]CIC nanoGUNE, 20018 Donostia – San Sebastian, Spain
[2]Max-Planck-Institut für Biochemie and Center for NanoScience, 82152 Martinsried, Germany
[3]FOM Institute for Atomic and Molecular Physics AMOLF c/o Philips Research Laboratories, 5656 AE Eindhoven, The Netherlands
[4]Materials innovation institute, 2628CD Delft, The Netherlands
[5]Institute for Molecules and Materials, Solid State Chemistry Department, Radboud University Nijmegen, 6525 ED Nijmegen, The Netherlands
[6]Philips Research Laboratories, 5656 AE Eindhoven, The Netherlands
j.stiegler@nanogune.eu

Semiconductor nanowires have gained tremendous interest in recent years due to their promising electronic and opto-electronic properties [1, 2]. For the implementation of semiconductor nanowires into devices it is crucial to precisely control the doping concentration of the nanowires. For tuning the fabrication process, new analytical tools are needed to quantitatively determine the doping concentration.

Dopants in single nanowires can already be measured using atom probe microscopy (APM) or transmission electron microscopy (TEM). But due to surface and shielding effects [3] not all dopants are ionized yielding a lower number of free-carriers. For the performance in electrical and opto-electronic devices the number of free carriers therefore is of utmost importance. Scanning-probe methods like scanning capacitance microscopy (SCM) and scanning spreading resistance microscopy (SSRM) can map the free-carriers. However, quantitative imaging is hardly achieved with SCM, and SSRM is a destructive method. Here we demonstrate that scattering-type scanning near-field optical microscopy (s-SNOM) can map free-carriers in single modulation-doped InP nanowires with nanoscale resolution, quantitatively and non-destructively.

s-SNOM offers an excellent optical resolution in the 10nm range independent of the wavelength [4] and allows for mapping the chemical composition [5], structural properties such as strain [6], and free-carriers in semiconductor devices [7]. It is typically based on atomic force microscopy (AFM) where the tip is illuminated with a focused laser beam and the tip-scattered light is detected simultaneously to topography. Using metallic tips, the strong optical near-field interaction between tip and sample modifies the scattered light allowing for probing the local dielectric properties with nanoscale resolution. Unavoidable background contributions are suppressed by vertical tip oscillation at frequency Ω and subsequent higher-harmonic demodulation of the detector signal at $n\cdot\Omega$ with $n\geq 2$ [8]. Combining this higher harmonic demodulation with interferometric detection, background-free near-field optical amplitude s_n and phase φ_n contrast imaging is possible.

Using s-SNOM we study the free-carrier properties in single modulation-doped InP nanowires, which were grown using the vapor-liquid-solid (VLS) method. For s-SNOM imaging, the nanowires were mechanically transferred onto a silicon substrate. Figure 1 shows simultaneously recorded topography and IR images of a single nanowire. While the topography shows a homogeneous wire surface, the IR images reveal the differently doped wire segments. We also observe a material contrast between the InP wire and the gold particle. The latter is used to catalyze the wire growth. Within this

contribution we will discuss the contrast mechanisms as well as the sensitivity of s-SNOM to free-carrier properties.

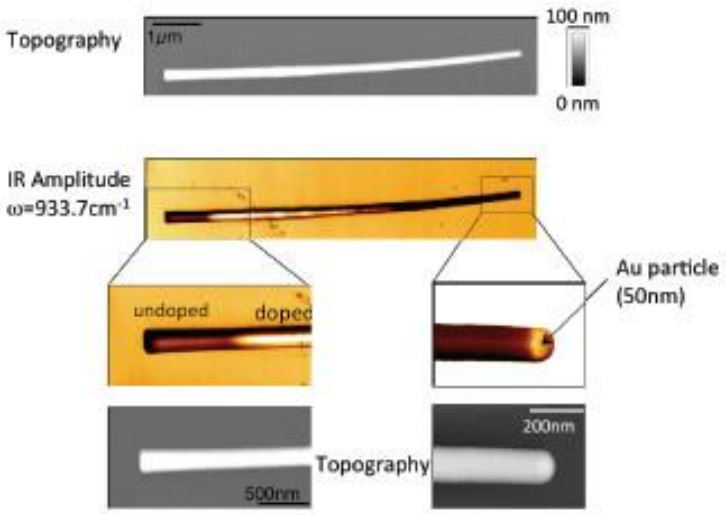

Figure1: *Topography and infrared amplitude s_2 of a representative InP nanowire recorded simultaneously at an IR laser frequency of 933.7cm^{-1} (10.71µm wavelength). The infrared images clearly reveal the differently doped nanowire sections and the material contrast between InP and the gold particle used to catalyze the nanowire growth.*

In conclusion, we demonstrate free-carrier profiling of individual doped InP nanowires. With s-SNOM we provide a contactless, non-destructive method, which allows quantitative local measurements of the free-carrier concentration in nanowires with nanoscale resolution. Improved modelling and spectral extension of s-SNOM to the THz frequency range could make the method a powerful tool for free-carrier profiling not only of nanowires, but also of other doped nanostructures and nanodevices.

References

[1] X. Duan, Y. Huang, R. Agarwal, and C. M. Lieber, Nature 421 (2003) 241
[2] M. H. Huang, S. Mao, H. Feick, H. Yan, Y. Wu, H. Kind, E. Weber, R. Russo, P. Yang, Science 292 (2001) 1897
[3] Y. M. Niquet, et al., Phys. Rev. B 73 (2006) 165319
[4] F. Keilmann, R. Hillenbrand, Phil. Trans. R. Soc. Lond. A 362 (2004) 787-805
[5] B. Knoll, F. Keilmann, Nature 399 (1999) 134-137
[6] A. Huber, A. Ziegler, T. Köck, R. Hillenbrand, Nat. Nanotech. advanced online publication (11. Jan. 2009) DOI10.1038/NNANO.2008.399
[7] A. Huber, D. Kazantsev, F. Keilmann, J. Wittborn, R. Hillenbrand, Adv. Mater. 19 (2007) 2209-2212
[8] N. Ocelic, A. Huber, R. Hillenbrand, Appl. Phys. Lett. 89 (2006) 101124

Noise properties of mesoscopic devices with realistic potential profile

M. Toraro, P. Marconcini, D. Logoteta and M. Macucci
Dipartamento di Ingegneria dell'Informazione, Via Caruso 16, I-56122 Pisa, Italy
E-mail: massimo.totaro@iet.unipi.it

The influence of disorder in mesoscopic structures on the value of shot noise suppression, i.e. on the Fano factor, has been the subject of significant research effort in the last two decades. Theoretical studies [1], [2], confirmed by numerical studies [3], [4] and experimental mesurements [5], have shown that the Fano factor should assume the value 1/3 if the conditions for diffusive trasport are reached.

This result has been theoretically found also for a series of tunnel barriers, using a semiclassical model [6]. However, using a numerical quantum-mechanical analysis based on a hard-wall approximation for the tunnel barriers, our group has recently found [7] that the 1/3 limit is not reached for a series of unevenly spaced ideal tunnel barriers, due to the presence of strong localization. Here we show that we obtain similar results also in the case of realistic tunnel barriers, since strong localization effects are preserved.

Another intriguing issue in this context is represented by the so-called "direct processes," i.e., events of direct transmission between the entrance and the exit constrictions of the cavity. These non-universal processes are expected to lead to a deviation from the additivity of constriction resistances and to a reduction of shot noise. Here we propose a cavity layout (see Fig. 3) that should allow an experimental verification of the properties of direct processes.

We have considered GaAs/AlGaAs heterostructures with the 2-dimensional electron gas (2DEG) at a depth d from the surface and we have studied devices defined by means of depletion gates in the 2DEG. For a fast but reasonable estimation of the confinement potential at the 2DEG level without solving the complete self-consistent problem (which would involve too heavy a computational burden for large parameter scans), we have used a technique based on the semianalytical evaluation of the potential, with the inclusion of screening from the charge in the 2DEG [8]. To increase the computational efficiency, we have reduced the number of transverse slices used for the discretization by merging adjacent slices with similar potential. Then we have computed the transmission matrix t of the structure using the recursive Green's function technique and we have found the conductance G and the Fano factor γ in the device using the Landauer-Büttiker formalism.

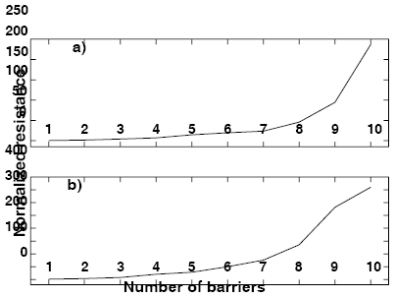

Figure 1: *Normalized resistance as a function of the number of barriers for ideal gates all biased at -0.9 V (a) and for gates with edges roughness biased in a range from -0.5 V to 0.8 V (b).*

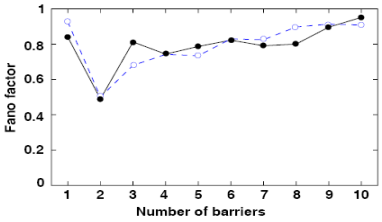

Figure 2: *Fano factor as a function of the number of barriers for ideal gates (solid line) and gates with edges roughness (dashed line).*

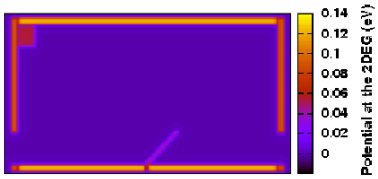

Figure 3: *Potential landscape at the 2DEG level for a mesoscopic cavity with a depletion gate at the upper left corner and a deflector gate in the middle of the bottom boundary of the cavity.*

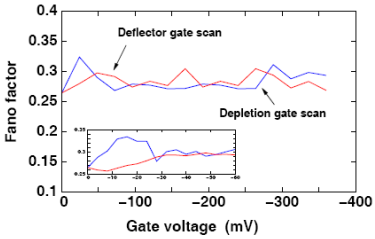

Figure 4: *Fano factor in the "quantum" regime of small cavity openings (split-gate gap: 250 nm). In the inset we show the behavior for small gate voltages.*

We show the numerical results we have obtained for a series of realistic tunnel barriers (in this case we have considered d = 50 nm). We have first generated the tunnel

barriers with ideal 20 nm wide unevenly spaced rectangular gates; the value of each interbarrier spacing has been randomly chosen between 500 nm and 520 nm. In order to obtain an average value, we have repeated our conductance and Fano factor calculations on 50 structures of this kind with different sets of interbarrier spacings and we have averaged over the 50 obtained results. Analogous calculations have then been performed introducing edge roughness in the gates defining the tunnel barriers. In particular, we have considered random deviations from the ideal rectangular shape in a range of ± 5 nm, with correlations between adjacent deviations, as in actual fabrication procedures. In the upper panel of Fig. 1 we show the results obtained for the resistance of a series of tunnel barriers defined with ideal gates, represented as a function of the number of barriers. In the lower panel of Fig. 1 we show a similar result for the resistance in the presence of edge roughness on the gates defining the barriers. The exponential behavior is a clear evidence of the presence of strong localization in the structure. In Fig. 2 instead we report the behavior of the Fano factor as a function of the number of barriers in the case of ideal gates (solid line) and gates with edge roughness (dashed line). In both cases, no 1/3 limit is observed for this structure and the behavior is quite similar to the one observed for hard-wall tunnel barriers [7].

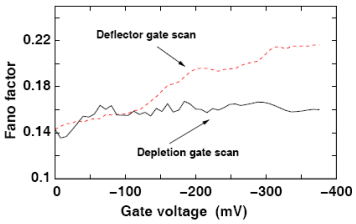

Figure 5: *Fano factor in the "classical" regime of large cavity openings (split-gate gap: 900 nm).*

We have also studied the noise properties of a mesoscopic cavity with tunable openings and gate voltages, the latter being located at different positions of the cavity (see Fig. 3; in this case d = 70 nm). We have considered a "depletion" gate located in the upper left corner of the cavity, and a so-called "deflector" gate, located in the middle of the bottom boundary of the cavity. Such a "deflector" gate can disrupt direct processes occurring between the two quantum point contacts. We have first focused on the "quantum" regime, with narrow constrictions that allow propagation of just a few transverse modes (N ≈ 3). Setting one of the two gates to zero voltage and tuning the other gate away from zero voltage, we have found slightly increased Fano factors (see Fig. 4): the two gates seemingly play analogous roles here. This behavior can be well understood by considering that in the "quantum" regime direct processes are strongly suppressed, but symmetry considerations become very important. In the "classical" regime of high mode numbers (N ≈ 34) the situation is quite different. Here we have found that activating the deflector gate systematically increases the noise (from F ≈ 0.14 to F ≈ 0.22), both in the case of an active and of an inactive depletion gate (the latter case is shown with the red dashed curve in Fig. 5). On the contrary, varying the depletion gate voltage affects the noise properties of the cavity only slightly (from F ≈ 0.14 to F ≈ 0.16) as shown in Fig. 5 (black solid curve). This behaviour nicely corresponds to a classical scattering picture in which direct trajectories between the openings are disrupted by the deflector gate but are left unchanged by the depletion gate.

In summary, we have numerically investigated the noise properties of different mesoscopic devices with a realistic potential profile. For a series of realistic tunnel barriers we have found that the strong localization effect is dominant. Finally, for a cavity with different tunable gates, we have investigated the role of direct processes in the "quantum" and in the "classical" regime.

References

[1] C. W. J. Beenakker and M. B¨uttiker, Phys. Rev. B, vol. 46, pp. 1889- 1892, 1992.
[2] K. E. Nagaev, Phys. Lett. A, vol. 169, pp. 103-107, 1992.
[3] A. Kolek, A. W. Stadler, and G. Halda´s, Phys. Rev. B, vol. 64, pp. 075202-1–5, 2001.
[4] M. Macucci, G. Iannaccone, G. Basso, and B. Pellegrini, Phys. Rev. B, vol. 67, pp. 115339-1–6, 2003.
[5] M. Henny, S. Oberholzer, C. Strunk, and C. Schönenberger, Phys. Rev. B, vol. 59, pp. 2871-2880, 1999.
[6] M. J. M. de Jong and C. W. J. Beenakker, Phys. Rev. B, vol. 51, pp. 16867-16870, 1995.
[7] P. Marconcini, M. Macucci, G. Iannaccone, and B. Pellegrini, Phys. Rev. B, vol. 79, 241307(R)-1–4 (2009).
[8]J. H. Davies, I. A. Larkin, and E. V. Sukhorukov, J. Appl. Phys., vol. 77, pp. 4504-4512, 1995.

Theoretical study of ptcda molecules adsorbed on InSb(001) surface

Dawid Toton
Department of Physics of Nanostructures and Nanotechnology, Institute of Physics, Jagiellonian University, Poland

Experimental STM studies of PTCDA molecules deposited on InSb(001) surface with c(8x2) reconstruction resulted in interesting pictures of molecular chains.
Their arrangement and orientation of individual molecules was unclear. To solve this problem, numerous DFT searches and optimizations were performed.
They enabled successful description of observed adsorption sites.
The theoretical work unveiled also an interesting interplay between dimensions of the molecule and surface geometry, which leads to highly anisotropic diffusion. The process is controlled by a pattern of chemical bond formation sites.

Supertransmission and light concentration at nanoscale

Francisco Javier Valdivia-Valero
ICMM-CSIC
C/Sor Juana Inés de la Cruz, 3 (Campus de Cantoblanco)
Madrid, Spain

This work deals with a combination of two subjects in nanophotonics: one is the phenomenon of anomalous transmission, or supertransmission, through a subwavelength slit; the other pertains to light concentration inside dielectric particles by excitation of morphology-dependent resonances (MDR) as either whispering gallery modes (WGM) or localised plasmons (LP).

In this study we address particles of nanometric size and show computer simulation results in the near field range. In order to observe supertransmission by a nanoslit in a metallic slab, we consider p-polarised light. Both the wavelength and the aperture width are adjusted so that the supertransmitted wave also excites the MDRs of nanoparticles in front of the aperture.

Results show enhancements of transmission much larger than from the slit alone, and concentration of both WGM and LP in the particles for these configurations. This suggests that the excitation of these resonances produce giant “extraction” of light through apertures, and it is associated to large intensity concentrations of both WGMs and LPs. Therefore such nanoparticles act as a switch for light. Several configurations of particle sets are considered.

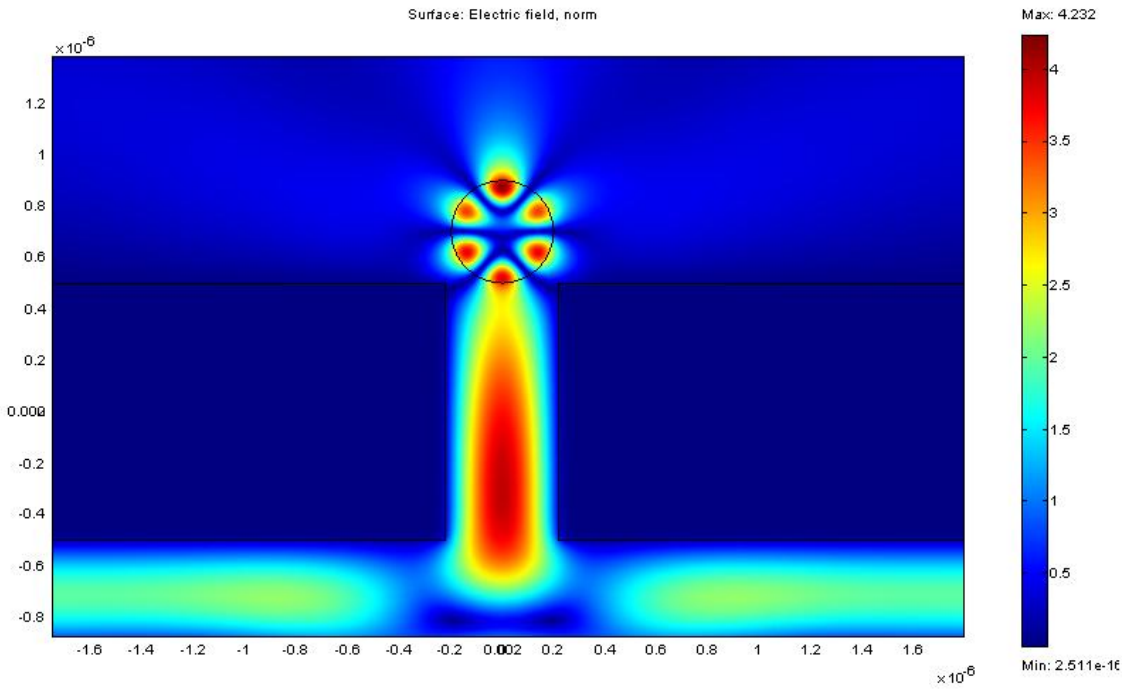

Towards near field characterization of plasmonic and magnetoplasmonic nanostructures

A. Vitrey[1], E. Ferreiro-Vila[1], A. García-Martín[1], M. U. González[1], J.M. García-Martín[1]

[1] Instituto de Microelectrónica de Madrid, IMM-CNM-CSIC, 28760-Tres Cantos, Spain
alan.vitrey@imm.cnm.csic.es

Most plasmonic devices are passive devices since their electromagnetic properties depend mainly on the shape of the structures, on the constitutive material of these structures and on the dielectric media. All those characteristics are generally fixed and the optical properties cannot be changed. A way to turn plasmonic devices into active ones is to use ferromagnetic metals, since the magneto-optical (MO) activity of these ferromagnetic metals is responsible for the modification of the optical response when applying an external low magnetic field. Unfortunately, plasmon resonances are critically broadened in ferromagnetic materials due to their important electromagnetic losses. An alternative is to combine ferromagnetic materials with noble metals. Recently, it has been demonstrated that Au/Co/Au nanodisks exhibit magnetoplasmonic properties such as a significant increase of the MO activity when the localized surface plasmon (LSP) resonance is excited [1,2].

Understanding the interplay between the LSP excitation and the MO activity is relevant from both fundamental and technological point of view. A path to this comprehension is to correlate the behavior of the LSP induced electromagnetic field and the MO activity. It has been clearly shown that the increase of MO activity is related to the enhancement of electromagnetic field penetrating into the Co layer [2]. In that way, the goal of this work is to characterize the distribution of the near field at the surface of the magnetoplasmonic structures as a function of their morphologies but also as a function of the position and the size of the ferromagnetic layer. This study will be achieved by combining the method of Scanning Near field Optical Microscopy in collection and illumination configurations with MO characterization. The lasers used to perform near field experiments and the LSP resonance of structures must have their wavelength close enough to couple efficiently the light with the LSP. Since the LSP wavelength is sensitive to the size of the nanostructures, the first step of this work has consisted in varying dimensions of the structures and carrying extinction spectrometry. Preliminary results have been obtained for Au dimers, nanorods and both Au and Au/Co/Au nanodisks, and then compared to other results presented by previous theoretical and experimental studies [3-5].

References

[1] J. B. González-Díaz et al., Small, 4, 202-205 (2008)
[2] G. Armelles et al., Opt. Express, 16, 16104-16112 (2008)
[3] T. Atay et al., Nano Lett., 4, 1627-1631 (2004); I. Romero et al., Opt. Express, 14, 9988-9999 (2006); S. S. Acimovic et al., ACS Nano, 3, 1231-1237 (2009)
[4] G. Laurent et al., Phys. Rev. B, 71,045430 (2005)
[5] G.W. Bryant et al., Nano Lett., 8, 631-636 (2008)

List of participants

Alphabetical Order

Participants – School 1 (NanoOptics and NanoPhotonics) (33)

Surname	Name	Institution	Country
Aizpurua	**Javier**	DIPC	Spain
Anttu	**Nicklas**	Lund University	Sweden
Aparicio Rebollo	**Francisco Javier**	Instituto de Ciencias de Materiales de Sevilla	Spain
Carminati	**Remi**	ESPCI	France
Cazé	**Alexandre**	ESPCI CNRS	France
Douas	**Maysoun**	ICMM-CSIC	Spain
Fernández Torrado	**Jorge**	Instituto de Microelectrónica de Madrid (CNM-CSIC)	Spain
Froufe	**Luis**	ICMM-CSIC	Spain
García López	**Oscar**	FideNa	Spain
Garcia Martinez	**Yamila**	Institut Catala de Nanotecnología	Spain
Hillenbrand	**Rainer**	CIC nanoGUNE Consolider	Spain
Inclán-Sánchez	**Luis**	Univesidad Autónoma de Madrid	Spain
Kaldirim	**Melih**	IMM-CNM-CSIC	Spain
Kandaswamy	**Prem Kumar**	INAC/SP2M/NPSC, CEA-Grenoble	France
Khan	**Abid Ali**	CIC nanoGUNE Consolider	Spain
Large	**Nicolas**	Centro Mixto de Física de Materiales CSIC-UPV/EHU & DIPC	Spain
Leconte	**Nicolas**	Université Catholique de Louvain (UCL)	Belgium
Muñoz	**Luis Enrique**	IMM-CNM-CSIC	Spain
Mupparapu	**Rajeshkumar**	European Laboratory for Nonlinear spectroscopy	Italy
Papencordt	**David**	University of Mainz	Germany
Pérez-González	**Olalla**	DIPC - University of the Basque Country	Spain
Saenz	**Juan Jose**	Universidad Autonoma de Madrid	Spain
San Sebastian	**Eneko**	CIC nanoGUNE Consolider	Spain
Sánchez Valencia	**Juan Ramón**	Consejo Superior de Investigaciones Científicas	Spain
Schnell	**Martin**	Asociación CIC nanoGUNE	Spain
Stiebeiner	**Ariane**	University of Mainz	Germany
Stiegler	**Johannes**	CIC nanoGUNE	Spain
Valdivia-Valero	**Francisco Javier**	ICMM-CSIC	Spain
van Hulst	**Niek**	ICFO	Spain
Vincent	**Remi**	DIPC	Spain
Vitrey	**Alan**	IMM-CNM-CSIC	Spain
Vivekananthan	**Radhalakshmi**	University of Florence	Italy
Yang	**Hongxin**	spintec/CNRS	France

Participants – School 2 (Modeling) (25)

Surname	Name	Institution	Country
Alarcón Pardo	**Alfonso**	Universitat Autonoma de Barcelona (UAB)	Spain
Albareda	**Guillem**	Enginyeria Electrònica	Spain
Brumme	**Thomas**	TU Dresden	Germany
Castanié	**Fabien**	CEMES-CNRS	France
de Oliveira	**Thales**	CIC nanoGUNE Consolider	Spain
Foti	**Giuseppe**	DIPC	Spain
García López	**Oscar**	FideNa	Spain
Godlewski	**Szymon**	Jagiellonian University	Poland
Gutierrez	**Rafael**	Dresden University of Technology	Germany
Kandaswamy	**Prem Kumar**	INAC/SP2M/NPSC, CEA-Grenoble	France
Khan	**Abid Ali**	CIC nanoGUNE Consolider	Spain
Landman	**Uzi**	Georgia Tech	United States
Large	**Nicolas**	Centro Mixto de Física de Materiales CSIC-UPV/EHU & DIPC	Spain
Leconte	**Nicolas**	Université Catholique de Louvain (UCL)	Belgium
Li	**Wu**	TU Dresden	Germany
Macucci	**Massimo**	Pisa University	Italy
Manrique	**Pedro David**	TU Dresden / Material sciences	Germany
Niquet	**Yann-Michel**	CEA/INAC	France
Nuansing	**Wiwat**	CIC nanoGUNE Consolider	Spain
Ordejon	**Pablo**	CIN2	Spain
Padilla	**José Luis**	Universidad de Granada	Spain
Pérez Osorio	**Miguel Angel**	Centre D'Investigació en Nanociència i Nanotecnologia (CIN2: CSIC-ICN)	Spain
Roche	**Stephan**	CEA-INAC	France
Totaro	**Massimo**	University of Pisa	Italy
Toton	**Dawid**	Jagiellonian University	Poland

Participants - nanoICT Symposium (57)

Surname	Name	Institution	Country
Aizpurua	**Javier**	CSIC - UPV/EHU - DIPC	Spain
Alarcón Pardo	**Alfonso**	Universitat Autonoma de Barcelona (UAB)	Spain
Albareda	**Guillem**	Enginyeria Electrònica	Spain
Anttu	**Nicklas**	Lund University	Sweden
Aparicio Rebollo	**Francisco Javier**	Instituto de Ciencias de Materiales de Sevilla	Spain
Bittner	**Alexander**	CIC nanoGUNE	Spain
Brumme	**Thomas**	TU Dresden	Germany
Campillo	**Igor**	CIC nanoGUNE	Spain
Carminati	**Remi**	ESPCI	France
Cazé	**Alexandre**	ESPCI CNRS	France
Correia	**Antonio**	Phantoms Foundation	Spain
de Oliveira	**Thales**	CIC nanoGUNE Consolider	Spain
Douas	**Maysoun**	ICMM-CSIC	Spain
Fernández Torrado	**Jorge**	Instituto de Microelectrónica de Madrid (CNM-CSIC)	Spain
Froufe	**Luis**	ICMM-CSIC	Spain
García López	**Oscar**	FideNa	Spain
Garcia Martinez	**Yamila**	Institut Catala de Nanotecnologia	Spain
Garcia-Martin	**Antonio**	Instituto de Microelectronica de Madrid - CSIC	Spain
Godlewski	**Szymon**	Jagiellonian University	Poland
Gutierrez	**Rafael**	Dresden University of Technology	Germany
Hillenbrand	**Rainer**	CIC nanoGUNE Consolider	Spain
Hueso	**Luis**	CIC nanoGUNE	Spain
Inclán-Sánchez	**Luis**	Univesidad Autónoma de Madrid	Spain
Kaldirim	**Melih**	IMM-CNM-CSIC	Spain
Kandaswamy	**Prem Kumar**	INAC/SP2M/NPSC, CEA-Grenoble	France
Khan	**Abid Ali**	CIC nanoGUNE Consolider	Spain
Landman	**Uzi**	Georgia Tech	United States
Large	**Nicolas**	Centro Mixto de Física de Materiales CSIC-UPV/EHU & DIPC	Spain
Leconte	**Nicolas**	Université Catholique de Louvain (UCL)	Belgium
Li	**Wu**	TU Dresden	Germany
Manrique	**Pedro David**	TU Dresden / Material sciences	Germany
Muñoz	**Luis Enrique**	IMM-CNM-CSIC	Spain
Mupparapu	**Rajeshkumar**	European Laboratory for Nonlinear spectroscopy	Italy
Niquet	**Yann-Michel**	CEA/INAC	France
Nuansing	**Wiwat**	CIC nanoGUNE Consolider	Spain
Ordejon	**Pablo**	CIN2	Spain
Papencordt	**David**	University of Mainz	Germany
Pérez Osorio	**Miguel Angel**	Centre D'Investigació en Nanociència i Nanotecnologia (CIN2: CSIC-ICN)	Spain
Pérez-González	**Olalla**	DIPC - University of the Basque Country	Spain
Roche	**Stephan**	CEA-INAC	France
Roldan Hernandez	**Jose Luis**	Phantoms Foundation	Spain
Saenz	**Juan Jose**	Universidad Autonoma de Madrid	Spain
San Sebastian	**Eneko**	CIC nanoGUNE Consolider	Spain
Sánchez	**Guillermo**	Centro de Tecnología Nanofotónica de Valencia	Spain
Sanchez Portal	**Daniel**	CSIC - UPV/EHU - DIPC	Spain
Sánchez Valencia	**Juan Ramón**	Consejo Superior de Investigaciones Científicas	Spain

Surname	Name	Institution	Country
Schnell	**Martin**	Asociación CIC nanoGUNE	Spain
Stiebeiner	**Ariane**	University of Mainz	Germany
Stiegler	**Johannes**	CIC nanoGUNE	Spain
Totaro	**Massimo**	University of Pisa	Italy
Toton	**Dawid**	Jagiellonian University	Poland
Valdivia-Valero	**Francisco Javier**	ICMM-CSIC	Spain
van Hulst	**Niek**	ICFO	Spain
Vincent	**Remi**	DIPC	Spain
Vitrey	**Alan**	IMM-CNM-CSIC	Spain
Vivekananthan	**Radhalakshmi**	University of Florence	Italy
Zabala	**Nerea**	Universidad del Pais Vasco	Spain

Sponsors

DONOSTIA INTERNATIONAL PHYSICS CENTER

nanoICT coordination action

CIC nanoGUNE nanoscience cooperative research center

Edited by

PHANTOMS foundation

Parque Científico de Madrid - Pabellón C - 1º Planta
Ctra. Colmenar Viejo Km. 15
Campus de Cantoblanco - Universidad Autónoma de Madrid
28049 Madrid - Spain
Fax +34 91 497 34 71
Email: antonio@phantomsnet.net
Web: http://www.phantomsnet.net